

Shape Variation in the Dermatocranium of the Greater Short-Horned Lizard *Phrynosoma hernandesi* (Reptilia: Squamata: Phrynosomatidae)

G. L. Powell¹ · A. P. Russell¹ · H. A. Jamniczky² · B. Hallgrímsson²

Received: 29 January 2016 / Accepted: 28 November 2016 / Published online: 28 December 2016
© Springer Science+Business Media New York 2016

Abstract Dermatocranial shape and horn morphology display great disparity among the species of *Phrynosoma*. Ontogenetic change in dermatocranial shape in a series of 79 specimens of the short-horned *Phrynosoma hernandesi* (54F: 25M) was examined using geometric morphometric techniques. A multivariate ANCOVA of Procrustes residuals with sex as a factor and ln(centroid size) as the covariate indicated sexual shape dimorphism. Separate multivariate regressions of Procrustes residuals on ln(centroid size) for each sex indicated that allometry accounts for ~52–54% of the total sample shape variance. Comparisons of ontogenetic shape change between sexes indicate that sexual shape dimorphism is minimal and of uncertain biological significance. Groupings of multivariate regression coefficients by magnitude and sign suggest that allometric integration of the dermatocranium is not uniform over the dermatocranium. Principal component analysis of the landmark configurations corrected for sex and allometry yields a first principal component which describes shape variance concentrated in the posterolateral and posterior regions of the dermatocranium, and again is indicative of non-uniform shape variation over the dermatocranium. Our findings for *P. hernandesi* indicate that the adult shape of

the dermatocranium may contribute to a passive defence against predation. We hypothesize that the complexity in dermatocranial shape demonstrated here for *P. hernandesi* indicates parcellation of shape variance, which may contribute to explanations of the pronounced dermatocranial disparity exhibited by the species of *Phrynosoma*.

Keywords Geometric morphometrics · Allometry · Sexual dimorphism · Integration

Introduction

The horned lizard genus *Phrynosoma* comprises 17 species that are distinguished from other members of the Phrynosomatidae by a unique suite of morphological, behavioural, and physiological traits (Pianka and Parker 1975; Sherbrooke 2003). *Phrynosoma* is characterized by a wide, short head and, ubiquitously, horns on the parietal, squamosals and frontal (Fig. 1). Some species also have horns (or hornlike asperities) on the jugals and postorbitals of the dermatocranium and the dentaries, surangulars and articulars of the mandible (Cope 1892; Bryant 1911; Smith 1946; Reeve 1952; Jollie 1960; Etheridge 1964; Jenkins and Tanner 1968; Presch 1969; Montanucci 1987; Baur and Montanucci 1998; Sherbrooke 2003). Horn morphology varies markedly within the genus (Fig. 1). Some species have long, pointed structures whereas others exhibit highly reduced ones (Reeve 1952; Presch 1969; Montanucci 1987; Baur and Montanucci 1998; Sherbrooke 2003; Leaché and McGuire 2006; Bergmann and Berk 2012). The dermatocranium of *Phrynosoma* is highly derived compared to that of the remainder of the Phrynosomatidae (Etheridge 1964; Presch 1969).

Electronic supplementary material The online version of this article (doi:10.1007/s11692-016-9403-6) contains supplementary material, which is available to authorized users.

✉ G. L. Powell
lpowell@ucalgary.ca

¹ Department of Biological Sciences, University of Calgary, 2500 University Dr. NW, Calgary, AB T2N 1N4, Canada

² Department of Cell Biology and Anatomy, Cumming School of Medicine, University of Calgary, 3330 Hospital Dr. NW, Calgary, AB T2N 4N1, Canada

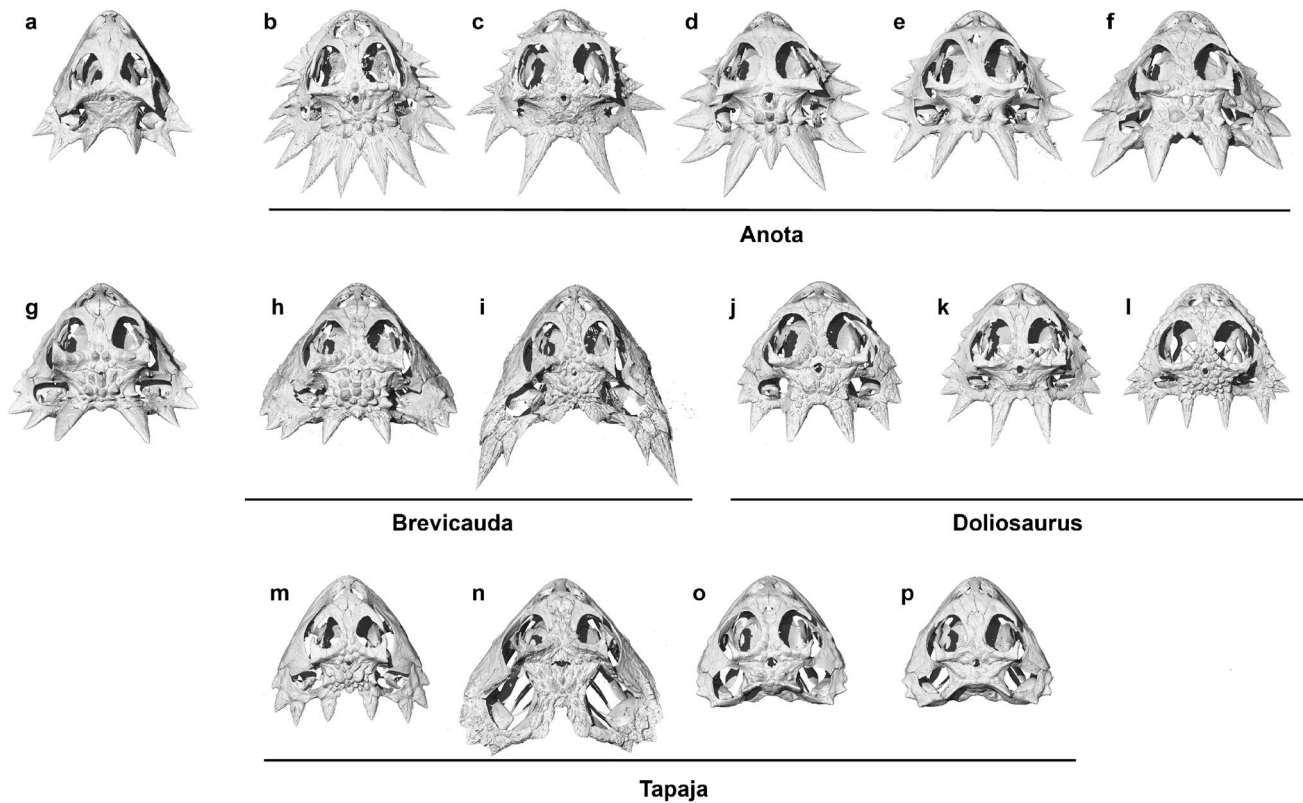


Fig. 1 Dorsal aspects of μ -CT scans of all species of *Phrynosoma* (except *P. sherbrookei*). Species grouped by crown clades of Leaché and McGuire (2006) and Leaché and Linkem (2015); horizontal black lines indicate clade membership. All specimens scaled to common distance between anterior tip of premaxilla and anterior margin of parietal foramen. **a** *P. asio* (CAS 132556), **b** *P. solare* (UM 67327), **c** *P. mcallii* (CAS 223630), **d** *P. coronatum* (CAS 143855), **e** *P. cerroense* (UCMVZ 182256), **f** *P. blainvilli* (UAZ 43866), **g** *P.*

cornutum (TCWC 30989), **h** *P. braconnieri* (UTACV 11392), **i** *P. taurus* (UTACVR 19393), **j** *P. platyrhinus* (CAS 37677), **k** *P. goodi* (CAS 229922), **l** *P. modestum* (TCWC 43872), **m** *P. orbiculare* (TCWC 54228), **n** *P. ditmarsii* (UAZ 32354), **o** *P. douglassii* (USNM 111352), **p** *P. hernandesi* (UA 280). Designations in parentheses following species names indicate the institution in which the specimen is curated, and its accession number (Online Resource, Section S.1)

The parietal and squamosal horns of *Phrynosoma* are thought to be important for defence in the longer-horned species (Pianka and Parker 1975; Sherbrooke 1991, 2003, 2008, 2013; Bergmann et al. 2009; Cooper and Sherbrooke 2010; Bergmann and Berk 2012), and have been shown to be so for some (Sherbrooke 1987, 2003; Young et al. 2004). Reduction in horn size co-occurs with viviparity; no long-horned species is viviparous and no short-horned species is oviparous (Baur and Montanucci 1998; Sherbrooke 2003; Leaché and McGuire 2006). A reduction in neonate horn size may facilitate parturition by reducing the possibility of damage to the female reproductive tract.

Bergmann and Berk (2012) investigated dermatocranial horn allometry in 14 species of *Phrynosoma*, and found that horns at different locations on the dermatocranium displayed interspecific variation in their patterns of allometric growth. The disparity in dermatocranial shape and horn morphology (Fig. 1) displayed among the species of *Phrynosoma* (Reeve 1952; Presch 1969; Montanucci 1987;

Baur and Montanucci 1998; Sherbrooke 2003; Leaché and McGuire 2006; Bergmann and Berk 2012) suggests that the cranial armature responds in complex ways to species-specific selection pressure. We predict, on this basis, that patterning of dermatocranial shape in the species of *Phrynosoma* is complex. Reduced morphological covariance among regions of the cranium, relative to the covariance within these regions, has been demonstrated for other lizards (Monteiro and Abe 1997; Bruner and Costantini 2007; Sanger et al. 2011, 2013; Lazić et al. 2015).

In dermatocranial shape, *Phrynosoma hernandesi* is typical of *Phrynosoma*, although its horns are highly reduced in size (Fig. 1p) relative to those of most of its congeners (Reeve 1952; Jollie 1960; Etheridge 1964; Jenkins and Tanner 1968; Presch 1969; Montanucci 1987; Baur and Montanucci 1998; Sherbrooke 2003; Leaché and McGuire 2006; Bergmann and Berk 2012). *P. hernandesi* is a member of the recently derived Tapaja clade (Fig. 1) within *Phrynosoma* (Leaché and McGuire 2006; Leaché and Linkem

2015), which shares a common ancestor with longer-horned clades within the genus. The short dermatocranial horns of *P. hernandesi* are thus regarded as a derived condition within the genus, but are homologous with those of the common horn suite displayed by all species (Fig. 1) of *Phrynosoma* (Bergmann and Berk 2012; Powell 2016). *P. hernandesi* thus presents a simplified exemplar of the *Phrynosoma* dermatocranium. The horns provide a contribution to the dermatocranial shape, but they will not have the overwhelming influence that the long horns of most congeners would exert.

The monophyly of *Phrynosoma hernandesi* was recently challenged by Montanucci (2015), who subdivided it into five species on the basis of external morphology. Until this is reconciled with molecular data (Zamudio et al. 1997), we retain the deployment of the more inclusive sense of *P. hernandesi* in this study, noting that the specimens we examine herein fall within Montanucci's (2015) *P. brevirostris*.

Geographic variation in orientation, length and spacing of the parietal and squamosal horns of *Phrynosoma hernandesi* is evident through assessments of external morphological traits (Smith 1946; Reeve 1952; Montanucci 1987, 2015), with the morphology of the parietal horns appearing to vary independently of that of the squamosal horns. Bergmann and Berk (2012) found that the parietal and squamosal horns of this species display significant positive allometry relative to snout-vent length (SVL), whereas the supraorbital horn on the frontal exhibits isometry. Regression slopes for horn length against body length were not greatly different from those for other species of *Phrynosoma* (Bergmann and Berk 2012).

The horns of *Phrynosoma hernandesi* are not known to be deployed actively in defence (Cope 1892; Smith 1946; Milne and Milne 1950; Sherbrooke 1987, 2003; Sherbrooke and Greenfield 2002; Sherbrooke et al. 2002), as they are in longer-horned species. They have not been shown to be used in any form of intraspecific display (the mating strategy of this species does not involve territoriality or agonistic encounter between males—Lynn 1965; Powell and Russell 1985a; Zamudio 1998; Bergmann and Berk 2012), and they are not used as gripping points by males during copulation (Montanucci and Baur 1982).

Jenkins and Tanner (1968) noted that the medial posterior emargination of the parietal of *Phrynosoma hernandesi* develops in the course of ontogeny, suggesting that shape change of the posterior portions of the squamosals and of the parietal are to some degree independent. The species displays significant sexual size dimorphism, males being markedly smaller than females at sexual maturity (Powell and Russell 1985a; Zamudio 1998). Growth models for the two sexes indicate that this is the result of a truncated growth trajectory in males, which attain sexual maturity earlier than females and cease growth at this point (Powell

and Russell 1985a). Ontogenetic increases in head width and head length display no allometric differences between males and females (Powell and Russell 1985a).

The lizard head is a complex structure, developmentally and structurally, and its shape is influenced by a variety of extrinsic and intrinsic factors (Kaliontzopoulou et al. 2008; Lazić et al. 2015). *Phrynosoma* exhibits a highly derived dermatocranium (Etheridge 1964; Presch 1969), divergent in morphology from those of most lizards (Jollie 1960; Evans 2008). It displays great dermatocranial disparity among its species (Fig. 1; Reeve 1952; Presch 1969; Montanucci 1987; Baur and Montanucci 1998; Sherbrooke 2003; Leaché and McGuire 2006; Bergmann and Berk 2012). We herein use geometric morphometric methods to characterize the shape of the dermatocranium and horns of *P. hernandesi*, a species with reduced horns and thus a relatively simple dermatocranial shape among its congeners (Fig. 1p), well-suited to be an exemplar of the genus in this regard. We first hypothesize that there is no difference in allometric trajectory of dermatocranial shape between males and females displayed by *P. hernandesi*. Adult male dermatocranial shape is produced by truncation of growth earlier in males than in females, along a common allometric trajectory. We hypothesize that changes in dermatocranial shape over the ontogenetic size range are produced by a non-uniform allometry, producing differences among the various regions of the dermatocranium, in particular between its anterior (rostral) region and the posterior regions encompassing the squamosals and the posterior portion of the parietal. Finally, we hypothesize that, with the effects of allometry removed, *P. hernandesi* will exhibit shape variance that is unevenly distributed over the dermatocranium, indicating possible parcellation. The results of the current investigation provide a context for investigations of the evolution of dermatocranial shape within the genus *Phrynosoma* as a whole.

Methods and Materials

Sample

Our sample of 79 ethanol-preserved lizards (Fig. 2, 54F: 25M) was collected in Alberta and Saskatchewan and the specimens are curated in various museums across Canada (Online Resource, Section S.1). The sample encompasses the populations at the northern edge of the species' geographic distribution (Powell and Russell 1998; Montanucci 2015). Leung et al. (2014) found little genetic variation among these populations, and thus restricting our sample to specimens from this area will minimize possible variance due to local genetic differences. Montanucci (2015) documented geographic variation in dermatocranial

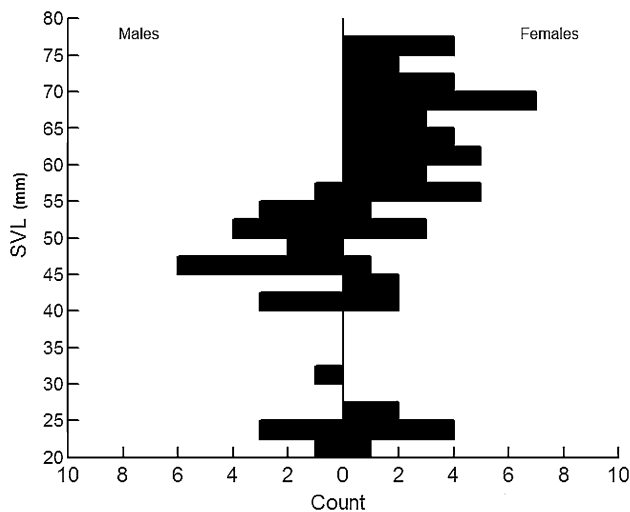


Fig. 2 SVL distributions of male and female *Phrynosoma hernandesi* used in this study

morphology over the wider geographic range of the species, but any effect of this is likewise eliminated by the geographical restriction of our sample. The final sample was arrived at after rejection of specimens exhibiting damage, and is used in all subsequent analyses (with the exception described immediately below).

Each specimen was sexed by application of the criteria provided by Powell and Russell (1985a) and Montanucci (2015). Neonate males display enlarged postanal scales and thereby can be accurately assigned to sex (Powell and Russell 1985a). Snout-vent length (SVL) was measured with a metal ruler to the nearest mm for each specimen (two desiccated specimens were too brittle for SVL measurements to be taken and had to be omitted from the analysis of the relationship between body size and dermatocranial centroid size—see below). Head length, from the base of the median parietal horn (P_1 , Fig. 3a, d) to the anterior tip of the rostrum, was taken to the nearest 0.1 mm with dial calipers (Mitutoyo model 505-633-50, Mitutoyo Canada Inc., Mississauga, Ont.). Body length was calculated as (SVL–head length) for each specimen.

We identified horns using the nomenclature employed by Powell et al. (2002) and Bergmann and Berk (2012). The medial parietal horn is designated as P_1 , the lateral parietal horns as P_2 , the squamosal horns (posterior to anterior) as S_1 , S_2 , and S_3 , and the horns on the lateral extremities of the transverse posterolateral processes of the frontal as F_0 (Fig. 3a–d).

Scanning

All specimens were scanned using a Scanco μ -CT 35 benchtop cone-beam microCT (SCANCO Medical AG,

Brüttsellen, Switzerland) in the Functional Imaging Lab, Department of Cell Biology and Anatomy, Cumming School of Medicine, University of Calgary. Scanning encompassed the region between the third or fourth cervical vertebra to 2 or 3 mm beyond the rostral tip of the premaxilla. The beam settings were 55 kVp, 72 μ A, at 4 W, with an integration time of 800 ms, resulting in a 1024×1024 voxel field of view. Voxel size ranged between 20.5 and 75.4 μm^3 , depending upon specimen size.

Visualization

All scan files were imported into Avizo[®] (Avizo[®] Standard Edition 7.0.1, FEI Visualization Sciences Group, Burlington, MA, USA) for reconstruction and visualization. For each specimen, an isosurface rendering was extracted and used for landmarking. Thresholds for retention of information were determined so as to simultaneously maximize definition of sutures and completeness of bone surface.

Adequate detail could not be resolved from a simple isosurface rendering for some specimens, because of either post-mortem mineralization of tissues immediately superficial to the surface of the dermatocranium, or incomplete ossification of the dermatocranial bones themselves. For these, a volumetric reconstruction was rendered, and the volumes containing the superficial material marked and subtracted from the total volume, so as to leave the dermatocranium unobscured. An isosurface for the desired volume was then generated and landmarked in the same manner as for the other specimens of the sample.

Head length, the straight-line distance from the anterior base of the median parietal horn (P_1 , Fig. 3a, d) to the anterior median tip of the premaxilla, was taken from the isosurface reconstruction of each specimen using the Avizo[®] 3D Measurement Tool, and this was compared to head length measured externally for the same specimen. This allowed checking for any discrepancies in the Avizo[®] reconstructions.

Landmarking

Landmarks were placed on dermatocranial isosurface reconstructions using Avizo[®]. All landmarks on all specimens were placed by the same individual (GLP). Technical issues relating to landmarking are described in the Online Resource (Section S.2). Three randomizations of the entire sample were performed; each of these determined schedules of landmarking sessions, separated by months. This minimized the possible effects of habituation on landmark placement error. The three sets of replicate landmark configurations were subjected to a Procrustes ANOVA in order to quantify measurement error in landmarking and

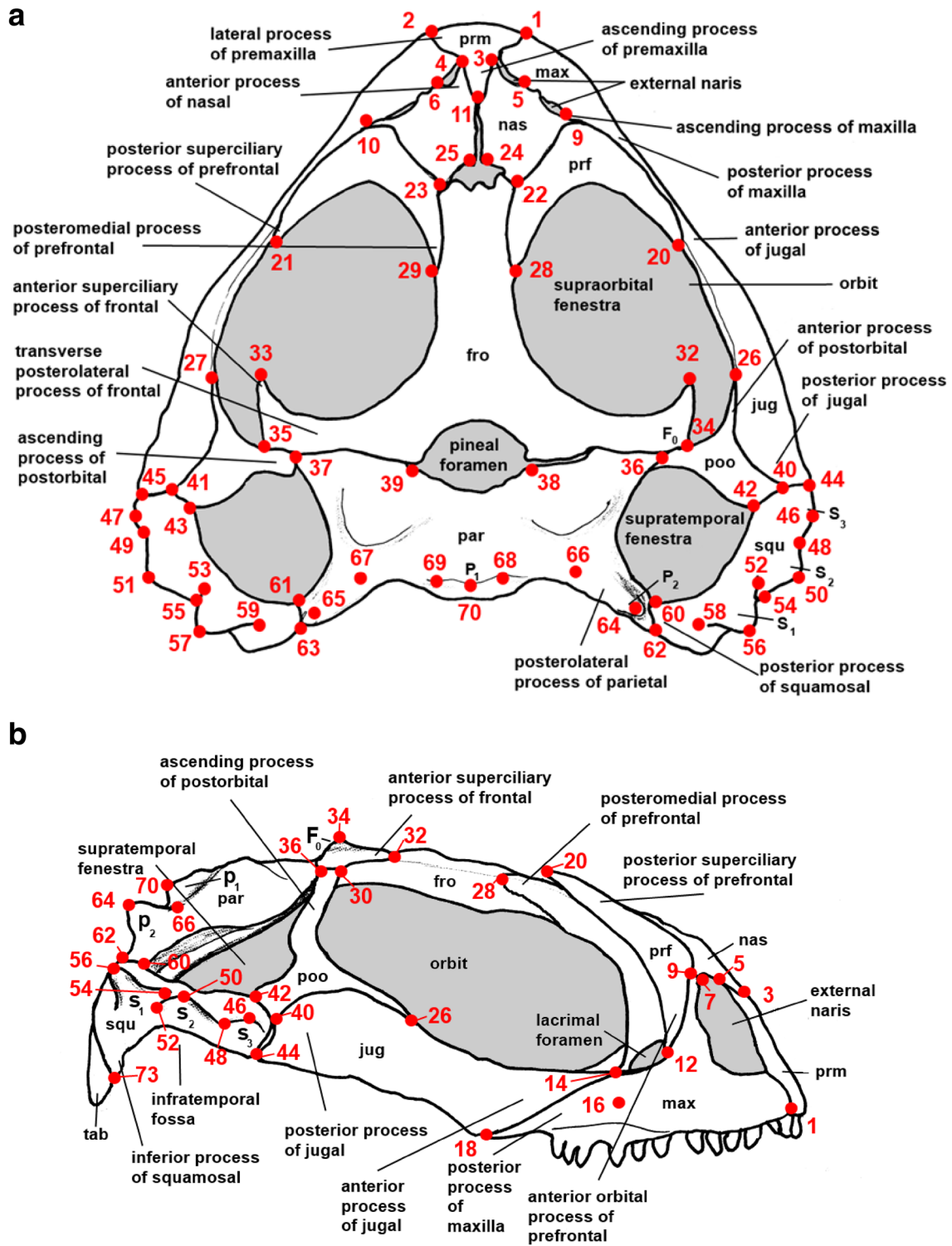


Fig. 3 Dermatocranium of *Phrynosoma hernandesi* in **a** dorsal view; **b** right lateral view; **c** anterior view; **d** posterior view. Abbreviations for bones: *fro* frontal, *jug* jugal, *max* maxilla, *nas* nasal, *par* parietal, *poo* postorbital, *prf* prefrontal, *prm* premaxilla, *squ* squamosal, *tab* tabular. Vertical hatching chondrocranial elements (supraoccipital).

Landmarks indicated and labelled in red; anatomical descriptions of placements given in Table 1. Squamosal horns (S_1 – S_3), parietal horns (P_1 , P_2), and supraorbital horn (F_0) indicated on right side (left side of **d**). Specimen pictured-UA 279; male; SVL 45 mm

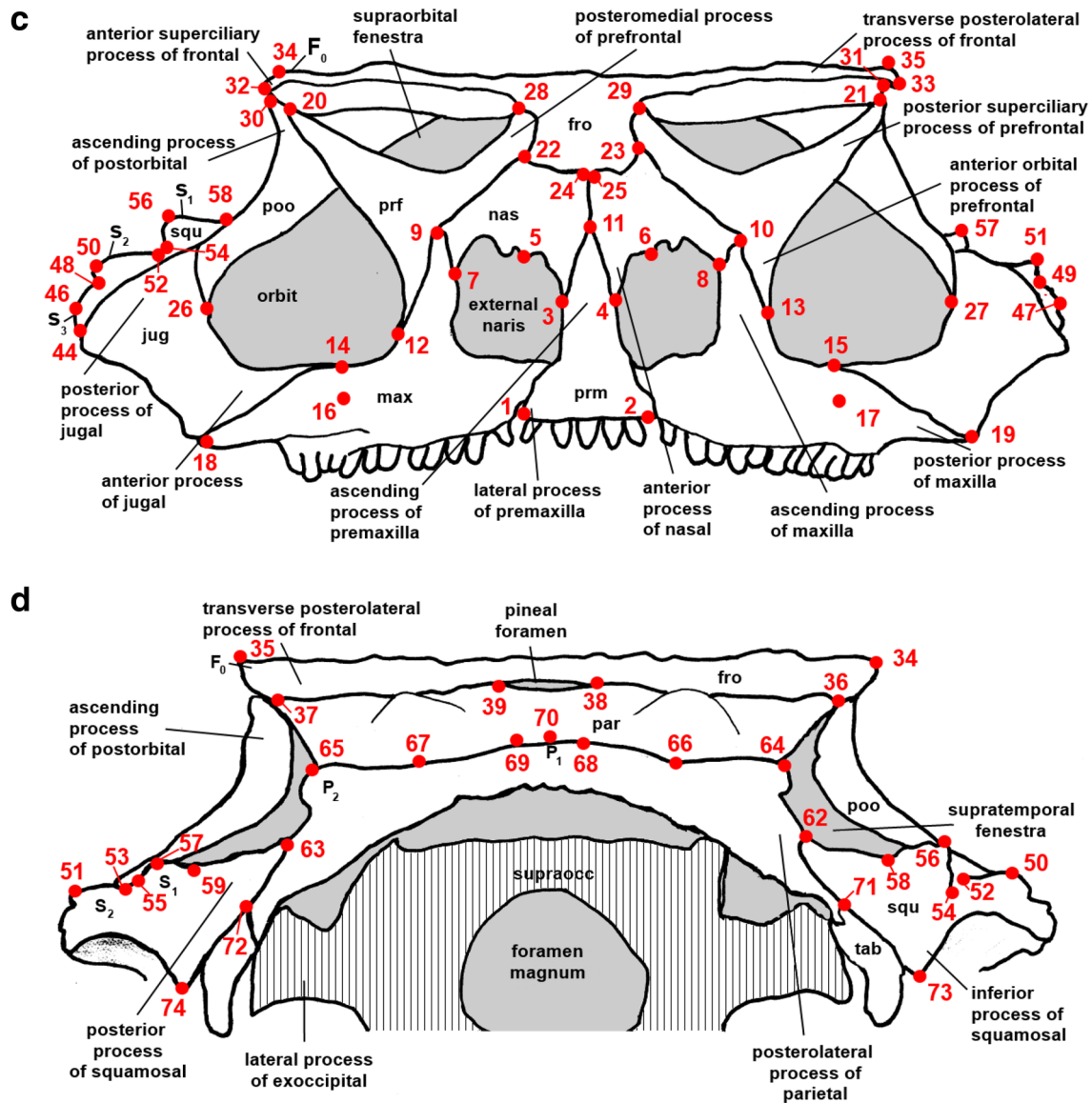


Fig. 3 (continued)

to examine variance due to asymmetry (see Section S.3, Online Resource).

Selection of Landmarks

The majority of the landmarks in the landmark configuration employed (Fig. 3; Table 1) identify termini or junctions of sutures (Bookstein’s Type 1 landmarks; Bookstein 1991; Zelditch et al. 2004). Landmarks were selected to provide a reasonable coverage of the dorsal and lateral aspects of the dermatocranium. Horns on the parietal, squamosal and frontal, important features of the genus, are not defined by sutures, and therefore are represented by Bookstein’s Type 2 landmarks (Bookstein 1991; Zelditch et al. 2004).

Analysis

Upon completion of the analysis of measurement error, which indicated that this was not a major source of variance in our statistical analysis (Online Resource, Table S-1), the mean landmark coordinates for each of the specimens were estimated from its three replicate landmark sets.

The entire sample was first subjected to a full Procrustes analysis, aligned by the principal axes of the mean configuration, in MorphoJ v.1.06d (Klingenberg 2011). The entire Procrustes shape coordinate sample was then examined for outliers by inspection of the cumulative squared Procrustes distance distribution of the entire sample, plotted against the expected cumulative distribution under the assumption

Table 1 Anatomical descriptions of landmark placements depicted in Fig. 3 (a–d)

Landmark number	Anatomical description of placement
1–2	Right and left lateral extremities of lateral processes of premaxilla
3–4	Inferior extremities of anterior processes of right and left nasals
5–6	Anterior extremities of processes extending from anterior margin of right and left nasals into right and left external nares
7–8	Inferior lateral extremities of nasal portions of margins of right and left external nares
9–10	Superior extremities of ascending processes of right and left maxillae
11	Superior extremity of ascending process of premaxilla
12–13	Inferior extremities of anterior orbital processes of right and left preorbitals
14–15	Anterior extremities of anterior processes of right and left jugals
16–17	Posteriormost margins of right and left posteriormost superior labial foramen
18–19	Posterior extremities of posterior processes of right and left maxillae
20–21	Posterior extremities of posterior superciliary processes of right and left preorbitals
22–23	Lateral posterior extremities of right and left nasals
24–25	Medial posterior extremities of right and left nasals
26–27	Anterior extremities of right and left postorbitals on inferior orbital margins
28–29	Posterior extremities of posteromedial processes of right and left preorbitals
30–31	Anterior extremities of ascending processes of right and left postorbitals
32–33	Anterior extremities of right and left anterior superciliary processes of frontal
34–35	Posterior superior extremities of right and left transverse posterolateral processes of frontal apices of superciliary horns (F_0)
36–37	Right and left anterolateral extremities of parietal
38–39	Right and left extremities of margin of pineal foramen, at level of parietofrontal suture
40–41	Junctions of inferior borders of right and left postorbitals, right and left posterior processes of jugals and right and left superior anterior processes of squamosals
42–43	Posterior ends of sutures between inferior margins of right and left postorbitals and medial margins of anterior processes of right and left squamosals
44–45	Anterior extremities of bases of right and left third squamosal horns (S_3)
46–47	Apices of right and left third squamosal horns (S_3)
48–49	Posterior extremities of bases of right and left third squamosal horns (S_3) and anterior extremities of bases of right and left second squamosal horns (S_2)
50–51	Apices of right and left second squamosal horns (S_2)
52–53	Posterior extremities of bases of right and left second squamosal horns (S_2)
54–55	Anterior extremities of bases of right and left first squamosal horns (S_1)
56–57	Apices of right and left first squamosal horns (S_1)
58–59	Medial extremities of bases of right and left first squamosal horns (S_1)
60–61	Anterior ends of suture between posterior processes of right and left squamosals and right and left posterolateral processes of parietal
62–63	Points at which suture between posterior processes of right and left squamosals and right and left posterolateral processes of parietal cross posterior border of cranium, at lateral base of right and left second parietal horns (P_2)
64–65	Apices of right and left second parietal horns (P_2)
66–67	Medial extremities of bases of right and left second parietal horns (P_2)
68–69	Right and left lateral extremities of base of median first parietal horn (P_1)
70	Apex of median first parietal horn (P_1)
71–72	Inferior extremities of right and left posterolateral processes of parietal
73–74	Inferior extremities of inferior processes of right and left squamosals

of multivariate normality. The distribution indicated some deviation from the expectations of multivariate normality (Online Resource, Fig. S-1), but does not display long tails, indicating that there are no replicates in the pooled data displaying large measurement errors. The symmetric portion of the total shape variation (Klingenberg et al. 2002;

Mitteroecker and Gunz 2009) was retained for further analyses; this removed possible variance due to developmental noise.

We investigated sexual dimorphism in the relationship between centroid size and body length in order to determine whether dermatocranial shape differed between the

sexes at a common body size. *Phrynosoma hernandesi* exhibits sexual size dimorphism over its geographical range, females exceeding males in adult snout-vent length (Powell and Russell 1984, 1985a; Zamudio 1998). Males in the Canadian populations attain a maximum SVL approximately 75% that of maximum female SVL (Fig. 2; Powell and Russell 1985a). This sexual size dimorphism in these populations has been shown to have intraspecific ecological significance, being associated with intersexual differences in the ranges of prey size taken (Powell and Russell 1984) and in thermal biology (Powell and Russell 1985b). An ecologically significant sexual size dimorphism could be associated with sexual dimorphism in dermatocranial shape at comparable body sizes. The allometric relationships of external head length and of external head width to SVL were shown not to differ significantly between the sexes in Alberta populations of this species (Powell and Russell 1985a); however, in the case of head length, the dependent variable was incorporated in the independent variable in these analyses, inflating the estimates of slope. Accordingly, we performed a least-squares ANCOVA of male and female $\ln(\text{centroid size})$, with $\ln(\text{body length})$ as the covariate, sex as a factor and an interaction term for sex and $\ln(\text{body length})$. There was no significant effect of sex ($F_{1, 73} = 0.4939$, $p=0.4844$) and no significant interaction between sex and $\ln(\text{body length})$ ($F_{1, 73} = 0.0001$, $p=0.9917$; see Online Resource, Fig. S-2, Table S-2). There is thus no difference between the sexes in the relationship between an ecologically significant index of overall body size and the measure of scale (Mitteroecker et al. 2013) used in subsequent geometric morphometric

analyses. We will be able to compare dermatocranial shapes between the sexes at the same centroid sizes and know that we are comparing shapes between lizards of the same body lengths.

We were not able to include location as a factor in this analysis. Due to the small sample sizes for all localities in Alberta and Saskatchewan, and the tendency of these samples to be biased towards one sex or the other, the effects of sex and location would have been conflated. Leung et al. (2014) found there to be little geographical genetic variation among the Canadian populations of *Phrynosoma hernandesi*, which suggests that location would not have contributed a great deal to the sample variance.

The analysis of allometric sexual dimorphism in centroid size (see above) did not allow us to assume that there were no significant sexual differences in allometry of dermatocranial shape. We thus subjected the symmetric portion of the Procrustes-fitted landmark configurations to a distance-based ANCOVA (Goodall 1991; Collyer et al. 2015) on $\ln(\text{centroid size})$, including terms for sex and the interaction between sex and $\ln(\text{centroid size})$, using the function *procD.allometry* from the R package *geomorph* v.2.1.6 (R Development Core Team 2013; Adams and Otárola-Castillo 2013; Adams et al. 2014).

The effect of sex was significant, and there was a significant interaction between sex and $\ln(\text{centroid size})$, for this regression (Table 2). The null hypothesis of parallel slopes was rejected ($F_{75, 77} = 2.637$; $p < 0.001$). The R^2 for sex (0.0194—Table 2) and for the interaction between $\ln(\text{centroid size})$ and sex (0.0104—Table 2) are both small compared to the R^2 for $\ln(\text{centroid size})$ (0.5465—Table 2).

Table 2 ANCOVA of symmetric portion of Procrustes-fitted landmark configuration, with $\ln(\text{centroid size})$ as covariate and sex as a factor

	df	SS	MS	R^2	F	Z	p
$\ln(\text{centroid size})$	1	0.153043	0.153043	0.54654	96.7524	23.7154	0.001
Sex	1	0.005432	0.005432	0.01940	3.4342	3.0860	0.002
$\ln(\text{centroid size}) \times \text{sex}$	1	0.002910	0.002910	0.01039	1.8394	1.7424	0.033
Error	75	0.118635	0.001582				
Total	78	0.280021					
Females ^a	df	SS	MS	R^2	F	Z	p
$\ln(\text{centroid size})$	1	0.10000	0.100004	0.54544	62.397	18.106	0.001
Error	52	0.08334	0.001603				
Total	53	0.18334					
Males ^b	df	SS	MS	R^2	F	Z	p
$\ln(\text{centroid size})$	1	0.039882	0.039882	0.52644	25.569	10.079	0.001
Error	23	0.035875	0.001560				
Total	24	0.075757					

^aRegression of female Procrustes-fitted landmark configurations on $\ln(\text{centroid size})$

^bRegression of male Procrustes-fitted landmark configurations on $\ln(\text{centroid size})$. Landmark configurations in (a) and (b) subject to common Procrustes fit

Residuals from this analysis were retained for subsequent analysis, and are henceforth referred to as the symmetric sex and allometry-free landmark data (SSAFL).

The existence of sexual dimorphism in the ontogenetic relationship between dermatocranial shape and $\ln(\text{centroid size})$ required that separate ontogenetic analyses for the sexes be performed. We thus divided the symmetric portion of the common Procrustes-fitted landmark configurations by sex, and performed separate multivariate regressions of the landmark configurations on $\ln(\text{centroid size})$ using MorphoJ v.1.06d (Klingenberg 2011). Shape changes over the ontogenetic size range of each sex were represented by wireframe diagrams, and by linear plots of regression coefficients for each of the x-, y-, and z-coordinates as continuous traces against landmark number (restricted to median landmarks and those on the right side of the dermatocranium). These allowed shape change due to allometry over the ontogenetic size range (Slice 2007; Klingenberg 2013; Mitteroecker et al. 2013) to be described more fully.

We based a principal components analysis of sex- and allometry-free shape upon the variance–covariance matrix that was generated from the SSAFL data. Criteria for retention of principal components are provided in Section S.4 of the Online Resource. The shape variation explained by each retained principal component was examined by inspection of wireframe diagrams of the dermatocranium, showing the deformations described by each principal component at the smallest and the largest of the scores of that principal component. We also plotted the principal component coefficients for each of the x-, y-, and z-coordinates as continuous traces against landmark number for each of the retained principal components, in order to better define spatially localized dermatocranial shape deformation explained by each principal component. Plots were restricted to the mid-line landmarks and those on the right side of the dermatocranium, to reduce crowding.

Results

Sample

Plots of predicted SVL changes over time in *Phrynosoma hernandesi* of both sexes from Alberta (based upon growth models generated from mark-recapture data) are given in Powell and Russell (1985a: Figs. 2, 4, 6). A comparison of the SVL distributions of the two sexes in the current sample (Fig. 2) to these plots (Powell and Russell 1985a: Figs. 2, 4, 6) indicates that although neonates, larger subadults and adults of both sexes are well-represented here, there is an almost complete absence of individuals representing the initial rapid phase of growth (~27–40 mm SVL—Fig. 2; Powell and Russell 1985a: Figs. 2, 4, 6). According to the

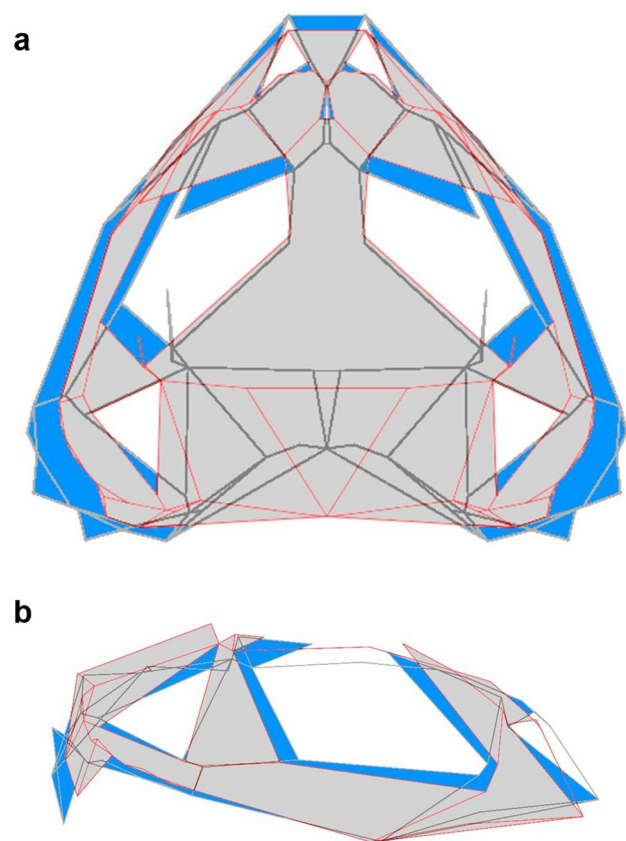


Fig. 4 Dorsal (a) and right lateral (b) wireframe reconstructions of dermatocranial shape predicted by multivariate regression of symmetric component of Procrustes-fitted landmark series of all female *Phrynosoma hernandesi* on $\ln(\text{centroid size})$. Shape at smallest $\ln(\text{centroid size})$ superimposed upon shape at largest $\ln(\text{centroid size})$ of sample; red wireframe with dark grey fill—at smallest $\ln(\text{centroid size})$ of sample; black wireframe with blue fill—at largest $\ln(\text{centroid size})$ of sample. Both shapes centred upon mean shape (not shown)

SVL growth models of Powell and Russell (1985a: Fig. 6) both sexes of recruits in a given year spend approximately 80 active days in the late summer and early fall of the year of birth, and spring and the earliest summer of the following active season (Powell and Russell 1985a: Figs. 2, 4), within this SVL range. Their rarity in museum collections appears to be due to collecting bias.

Males are difficult to age once they have entered their second year of growth (Powell and Russell 1985a: Figs. 2, 6), but the SVL distribution of males of >40 mm SVL in the sample provides good representation of older subadults (40–50 mm SVL) and adults (>50 mm SVL; Fig. 2). Females extend SVL growth through the third year after birth (Powell and Russell 1985a: Figs. 4, 6), and females >40 mm SVL in the sample can be divided into those in their first full year after year of birth (40–55 mm SVL), those in their second full year after birth (55–65 mm SVL), and those in their third full year after birth or older

(>65 mm SVL). All three of these size/age classes are well represented in the sample (Fig. 2). The sample is thus well-constituted for modelling ontogenetic changes in dermatocranial shape in both sexes of *Phrynosoma hernandesi*.

Overall sex ratios at birth are not skewed towards females (Powell and Russell 1991). The proportion of males to females presented in this sample (Fig. 2) is typical of Canadian field samples (Powell and Russell 1984, 1985a, b).

Ontogenetic Variation

The regressions of the symmetric portion of the landmark configurations on $\ln(\text{centroid size})$ were significant for both males and females (Table 2). R^2 values for females (0.545—Table 2) and males (0.526—Table 2) are similar; for both sexes, over 50% of the variance in the symmetric portion of dermatocranial shape can be explained by centroid size.

Wireframe plots of dermatocranial shape change over the ontogenetic size range of female *Phrynosoma hernandesi* (Fig. 4a, b) indicate that the anterior margin of the rostrum becomes slightly elevated and extended. The posterior superciliary processes of the prefrontals move medially, ventrally and posteriorly (Fig. 4a, b). The orbital margins of the jugals and of the postorbitals move dorsally and anteriorly, respectively, contributing to the relative reduction in orbit size (Fig. 4a, b). The anterior superciliary processes of the frontal move medially and extend further anteriorly (Fig. 4a, b), and increase in dorso-ventral depth (Fig. 4b). The medial movement of these processes accompanies the medial and anterior movements of the transverse posterolateral processes of the frontal and the lateral margins of the parietal (Fig. 4a). The ventro-lateral margins of the jugals, and the lateral and postero-lateral margins of the squamosals, become extended laterally and posterolaterally, accompanied by increases in squamosal horn size (Fig. 4a). The medial portion of the posterior margin of the parietal moves anteriorly relative to the posterolateral processes of the parietal, producing a marked medial emargination of the posterior margin of the dermatocranium (Fig. 4a). The dorsal surface of the cranial table moves ventrally, resulting in a depression of its dorsal surface relative to the transverse posterolateral processes of the frontal (Fig. 4b). The transverse posterolateral processes of the frontal, and the supraorbital horns (F_0) that they bear, thus become elevated relative to the cranial table (Fig. 4b). The apices of the paired parietal horns (P_2) become elevated, and their medial bases move medially and anteriorly with the medial margin of the posterior margin of the parietal (Fig. 4a, b). The inferior processes of the squamosals increase in relative size and ventral projection, and move posteriorly (Fig. 4b).

The shape changes over the ontogenetic size range of female *Phrynosoma hernandesi* thus consist primarily of depression of the posterior portion of the dermatocranium, together with lateral and posterolateral extension of the lateral and posterolateral margins of the squamosals, emargination of the posterior margin of the parietal, and elevation of the posterior margin of the frontal (Fig. 4a, b). Shape changes in the anterior portion of the dermatocranium consist predominantly of extension and elevation of the anterior tip of the rostrum (Fig. 4a, b). The squamosal, paired parietal, and supraorbital horns become relatively larger, and the anterior superciliary processes of the frontal and the posterior superciliary processes of the prefrontals move so as to occlude a greater proportion of the lateral margins of the supraorbital fenestrae (Fig. 4a, b).

Wireframe plots of dermatocranial shape change over the ontogenetic size range of male *Phrynosoma hernandesi* (Fig. 5a, b) indicate changes broadly similar to those observed in the female dermatocranium (Fig. 4a, b), although males do not attain the adult body size of females and these changes are not so marked. The elevation and anterior extension of the anterior tip of the rostrum at maximum male centroid size is more pronounced in males (Fig. 5a, b) than in females at maximum female centroid size (Fig. 4a, b), and there is slight lateral extension of the ventral margins of the maxillae in males (Fig. 5a, b), which is not seen in females (Fig. 4a, b). Other ontogenetic shape changes in the male dermatocranium (Fig. 5a, b) parallel those described for the female dermatocranium (Fig. 4a, b; see above), although not so pronounced, suggesting that the preponderance of ontogenetic shape changes in the dermatocrania of the sexes result from common growth processes.

A comparison of dermatocranial shape in males and females at the greatest centroid size attained by males, as determined by their respective regressions, reveals few differences (Fig. 6a, b). Males exhibit slightly greater anterior projection of the anterior margins of the prefrontal and nasals, and posterior displacements of the posterior margin of the frontal, anterior superciliary processes of the frontal and posterior margins of the postorbitals (Fig. 6a, b). Other sexual shape differences at this centroid size are negligible (Fig. 6a, b).

Although the coefficients of the multivariate regression of landmark position on $\ln(\text{centroid size})$ cannot be interpreted as allometric coefficients *sensu stricto*, examination of their relative magnitudes and signs gives some insight into the allometric shape changes illustrated in Figs. 4a, b and 5a, b. Plots of the regression coefficients for the x, y, and z coordinates for the median landmarks and those covering the right side of the dermatocranium for both sexes (Fig. 7a, b) indicate that allometric shape change is similar in both sexes of *Phrynosoma hernandesi*. Both plots suggest consonance of ontogenetic movements in the same

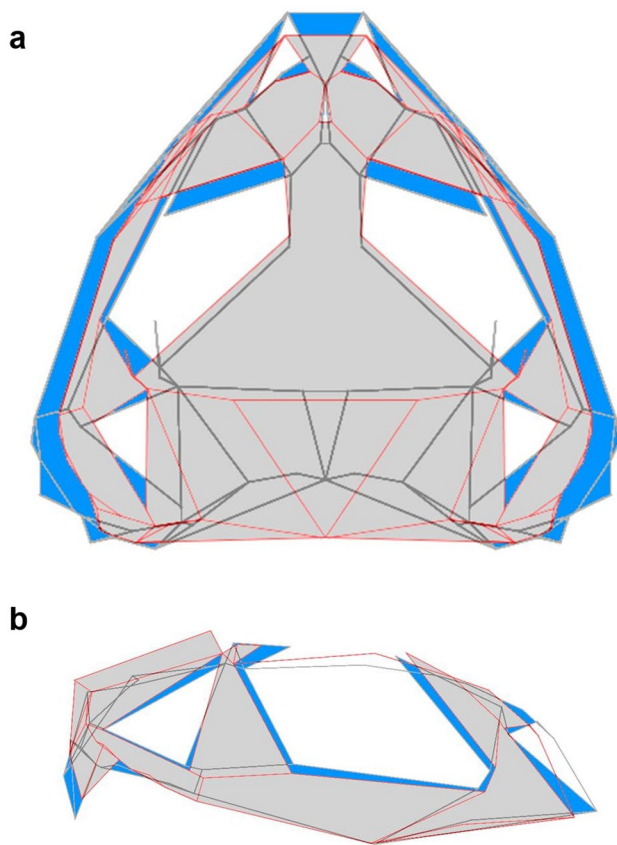


Fig. 5 Dorsal (a) and right lateral (b) wireframe reconstructions of dermatocranial shape predicted by multivariate regression of symmetric component of Procrustes-fitted landmark series of all male *Phrynosoma hernandesi* on $\ln(\text{centroid size})$. Shape at smallest $\ln(\text{centroid size})$ superimposed upon shape at largest $\ln(\text{centroid size})$; red wireframe with dark grey fill—at smallest $\ln(\text{centroid size})$ of sample; black wireframe with blue fill—at largest $\ln(\text{centroid size})$ of sample. Both shapes centred upon mean shape (not shown)

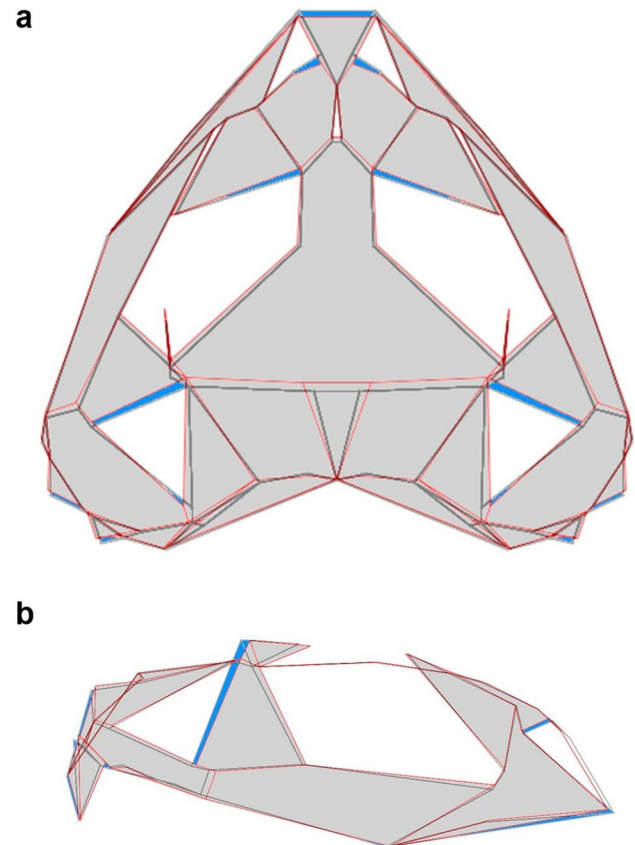


Fig. 6 Dorsal (a) and right lateral (b) wireframe reconstructions of dermatocranial shape predicted by multivariate regressions of symmetric component of Procrustes-fitted landmark configurations on $\ln(\text{centroid size})$ for females and males at greatest male $\ln(\text{centroid size})$. Female dermatocranial shape superimposed upon male dermatocranial shape; red wireframe with dark grey fill—female dermatocranial shape; black wireframe with blue fill—male dermatocranial shape. Both shapes centred upon common mean (not shown)

spatially localized groups of landmarks (Fig. 7a, b). The best defined of these are (Fig. 8): Landmarks 30–38, those covering the anterior portion of the parietal and posterior portion of the frontal (including the supraorbital horn- F_0 —Fig. 3a, b); Landmarks 40–56, those covering the anterior region and anterior lateral border of the squamosal, including horns S_3 and S_2 , and the apex of horn S_1 (Fig. 3a, b); Landmarks 60–66, those covering the posterior process of the squamosal and the posterolateral process of the parietal, including horn P_2 (Fig. 3a, b, d); Landmarks 68–70, situated medially on the posterior margin of the parietal (Fig. 3a, d); Landmarks 72–74, those covering the inferior process of the squamosal (Fig. 3b, d).

The landmarks covering the medial and lateral anterior portion of the rostrum (Landmarks 1–18; Fig. 3a–c; Table 1) do not display large values for the regression coefficients of their coordinates or marked regional coordinations of their signs (Fig. 6a, b).

The groupings of multivariate regression coefficients by propinquity, magnitude and sign on all three axes (see above; Figs. 7, 8) suggest that allometric integration of the dermatocranium is complex.

Symmetric Sex- and Allometry-Free Shape Variation

The first 36 principal components of the principal component analysis of the SSAFL data explained 95% of the total variance of the sample. The sample size is well in excess of this number of components, and so interpretation of the analysis is tenable (Klingenberg 2013).

Of the total set of components resulting from the principal component analysis of the residuals from the multivariate regression of landmark position of $\ln(\text{centroid size})$, the broken-stick criterion indicated that the first eight should be retained (expected percent of total variance for the ninth principal component = 2.910; observed percent of

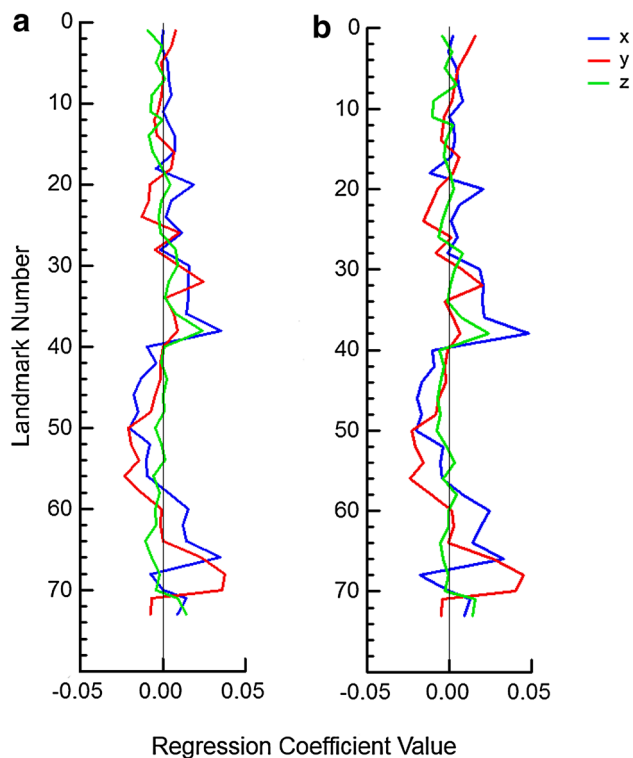


Fig. 7 Plot of multivariate regression coefficient values of x-, y-, and z- coordinates of landmarks against landmark number, for median landmarks and those upon the right side of the dermatocranium. **a** females; **b** males

total variance explained by PC9=2.670). Examination of the histogram of percent total variation explained by each component for all of the principal components of this analysis (Fig. 9), however, indicates a discontinuity in the rate of decrease of the amount of total variance explained at the transition between PC3 and PC4; the variance described by the PCs to the right of PC3 is not expected to be consequential. PC1–PC3 cumulatively explain 42.2% of the total variance, whereas PC4–PC8 explain 20.2% (Table 3). We therefore examined the variance in dermatocranial shape explained by PC1–PC3 in detail.

PC1 explains 24.287% of the allometry-free shape variation of the sample (Table 3). The main shape change described by PC1 is due to the relative dorso-ventral and medio-lateral movement of the region encompassing the anterior portions of the squamosals, the ventral portions of the postorbitals, and the posterior processes of the jugals (Fig. 10a, b). This results in a widening and dorso-ventral compression of the dermatocranium in the area defined by the anterior regions of the squamosals, the ventral portions of the postorbitals, and the posterior processes of the jugals (Fig. 10a), from smallest to largest PC1 score (Fig. 10b). The rostrum is depressed and abbreviated, its anterior tip displaced ventrally and posteriorly over the range from

smallest to greatest PC1 scores (Fig. 10a, b). The posterior ventral margins of the squamosals, bearing the inferior processes of the squamosals, are displaced anteriorly over this interval, resulting in an anterior movement of the posterolateral margins of the dermatocranium (Fig. 10a, b). The transverse posterior processes of the frontal do not experience great medio-lateral movement (Fig. 10a), but move dorsally. The anterior superciliary processes of the frontal become shorter, and their tips become elevated (Fig. 10a, b).

PC2 describes 10.133% of the total variance of the SSAFL sample, less than half of that described by PC1 (Table 3). Shape variation described by PC2 is associated with anterior projection of the anterior tip of the rostrum (Fig. 11a, b). At the lowest PC2 score, the anterior margin of the premaxilla is narrower and extends further anteriorly; at the highest PC2 score, the premaxilla as a whole is broader and shorter (Fig. 11a). Accompanying this is a posterior displacement of the anterior borders of the nasals at the highest PC2 score, and a depression of the dorsal surface of the rostrum as a whole (Fig. 11a, b). The transverse posterolateral processes of the frontal are elevated at the highest PC2 score, and the anterior margins of the postorbitals move anteriorly (Fig. 11b). The anterior margins of the squamosals move anteriorly, the posterior borders move slightly laterally, and the medial borders move dorsally; this is accompanied by lateral movements of the lateral margins of the parietal (Fig. 11a, b). The roof of the cranial table moves dorsally between the smallest and greatest PC2 scores, and the inferior squamosal processes move anteriorly (Fig. 11b).

PC3 explains 7.823% of the total variance of the SSAFL sample (Table 3). The shape changes accounted for by PC3 (Fig. 12a, b) are mainly associated with the degree of relative depression of the dorsal aspects of the post-rostral dermatocranium, and the degree of posterior extension of the posterior and ventral portions of the squamosals and lateral posterior margin of the parietal (Fig. 12a, b). The supraorbital horns (F_0) become less prominent with increasing PC3 score value (Fig. 12b). The orbital margins of the jugals move dorsally over the PC3 score range, and the posterior margins of the posterior superciliary processes of the prefrontals move posteriorly (Fig. 12a). The inferior processes of the squamosals move posteriorly and superiorly from least to greatest PC3 score, extending the posterolateral margins of the dermatocranium posteriorly (Fig. 12a, b). The roof of the frontal becomes depressed over the PC3 score range (Fig. 12b).

The plot of PC1 coefficients for the x, y and z coordinates for the landmarks covering the right side of the dermatocranium, and the unpaired median landmarks (Landmarks 11 and 70; Fig. 3a, c, d; Table 1) illustrates regional consonance of relative movement in changes

Fig. 8 Landmarks grouped by consonance of multivariate regression sign and progression for females (see Fig. 7a). *Red*—landmarks 30–38, those covering the anterior portion of the parietal and posterior portion of the frontal, including horn - F_0 ; *green*—landmarks 40–56, those covering the anterior region and anterior lateral border of the squamosal, including horns S_3 and S_2 , and the apex of horn S_1 ; *dark blue*—landmarks 60–66, those covering the posterior process of the squamosal and the posterolateral process of the parietal, including horn P_2 ; *light blue*—landmarks 68–70, situated medially on the posterior margin of the parietal; *gold*—landmarks 72–74, those covering the inferior process of the squamosal; *grey*—remaining, ungrouped landmarks

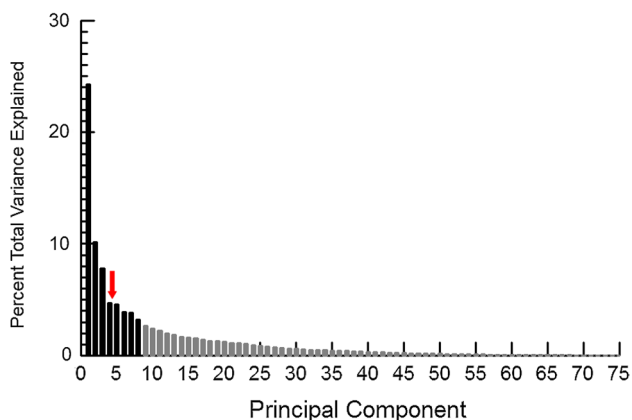
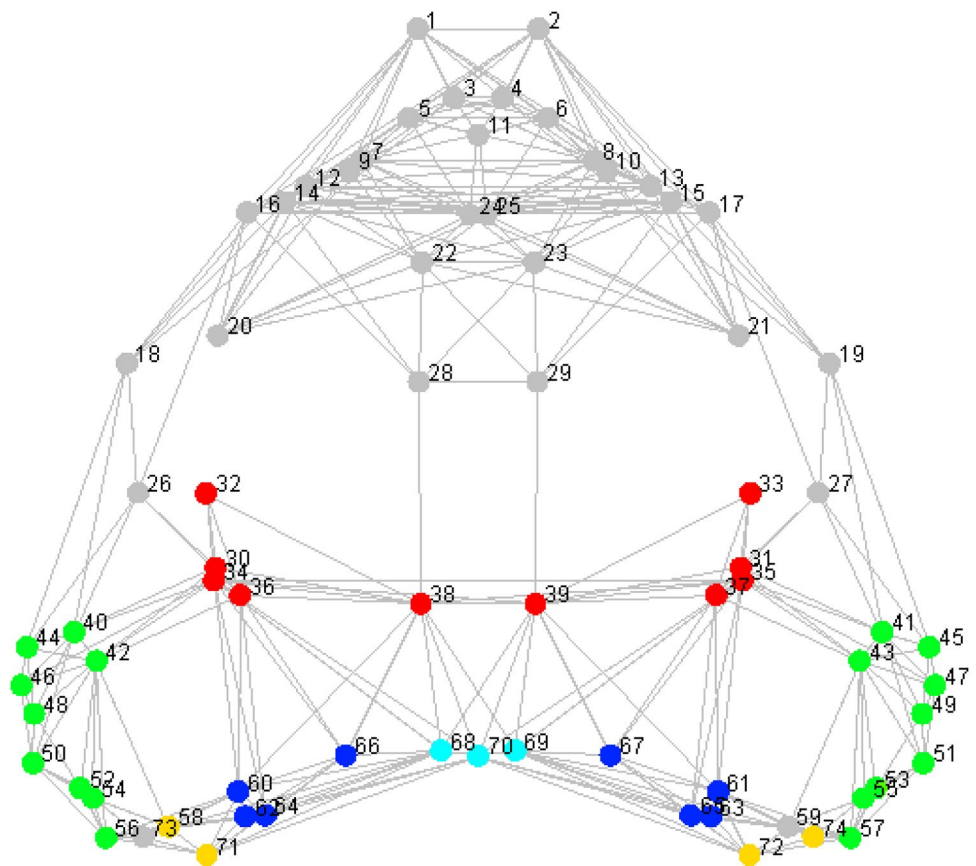


Fig. 9 Percent of total sample variance described by principal components from principal component analysis of SSAFL data. *Black bars* indicate components retained by application of the broken-stick criterion; *arrow* indicates discontinuity in rate of decrease of variance explained. Principal components to *left of arrow* retained for closer examination

in sign and magnitude of the PC1 coefficients from the anterior to posterior extremities of the dermatocranium (Fig. 10c). The plots of the PC2 and PC3 coefficients for the x-, y- and z-coordinates for these landmarks (Figs. 11c, 12c) likewise display consonance in sign and, to a lesser

Table 3 Eigenvalues, % total variance explained, and cumulative % variance explained for each of the first eight principal components of the principal component analysis of the SSAFL data for the *Phrynosoma hernandesi* sample retained according to broken-stick analysis

	Eigenvalue	% total variance explained	Cumulative % total variance explained
1	0.00037	24.287	24.287
2	0.00015	10.133	34.420
3	0.00012	7.823	42.243
4	0.00007	4.694	46.937
5	0.00007	4.586	51.522
6	0.00006	3.878	55.400
7	0.00006	3.826	59.226
8	0.00005	3.223	62.449

Bold indicates PCs discussed in detail in this study

degree, magnitude, that define groupings of landmarks which, while not corresponding exactly with one another or those defined by the coefficients of PC1 (Fig. 10c), broadly overlap with, and/or subdivide, these groupings. The portions of the total SSAFL variance in landmark position incorporated by each principal component are uncorrelated with each other. Thus, the groupings of landmarks by consonance of their principal component coefficients

Fig. 10 Dorsal (a) and right lateral (b) wireframe reconstructions of dermatocranial shape showing the shape changes associated with PC1 from principal component analysis of SSAFL data for *Phrynosoma hernandesi* sample. Shape at smallest PC1 value superimposed upon shape at largest PC1 value; red wireframe with dark grey fill—at smallest PC1 score of sample; black wireframe with blue fill—at largest PC1 score of sample. Both shapes centred upon mean shape (not shown). c Plot of PC1 coefficients of x-, y-, and z-coordinates of landmarks against landmark number, for median landmarks and those upon the right side of the dermatocranium

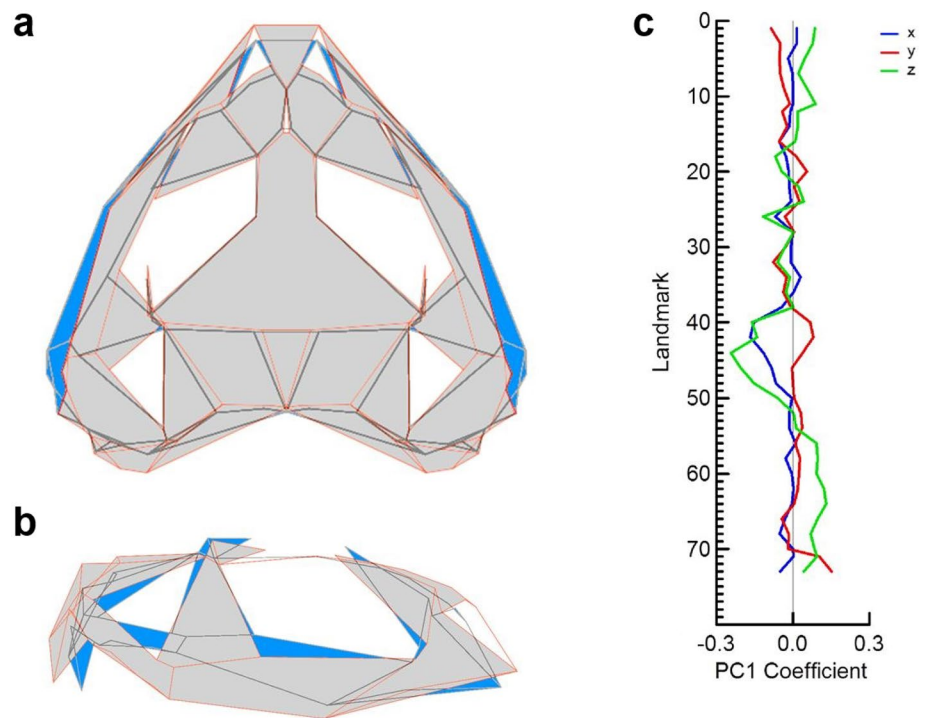
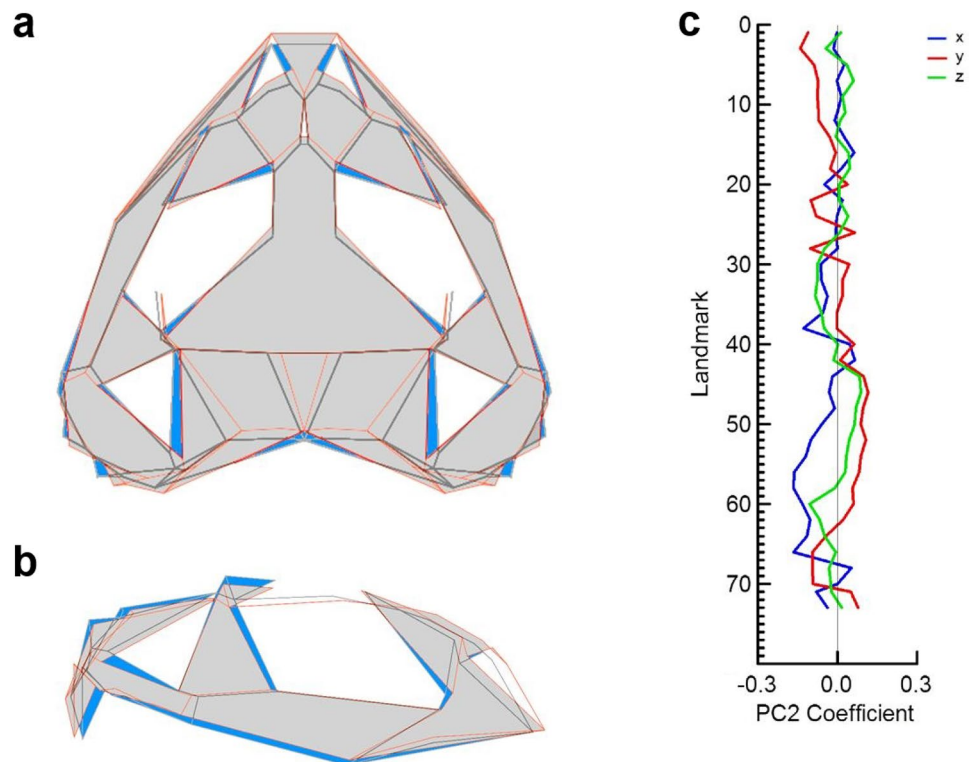


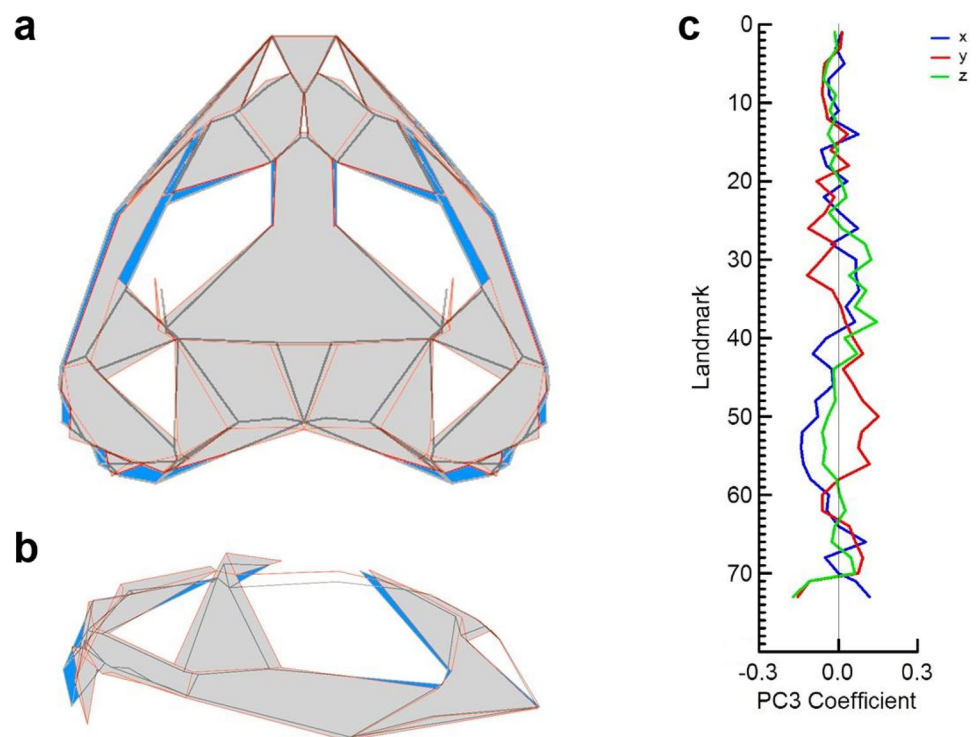
Fig. 11 Dorsal (a) and right lateral (b) wireframe reconstructions of dermatocranial shape showing the shape changes associated with PC2 from principal component analysis of SAFL data for *Phrynosoma hernandesi* sample. Shape at smallest PC2 value superimposed upon shape at largest PC2 value; red wireframe with dark grey fill—at smallest PC2 score of sample; black wireframe with blue fill—at largest PC2 score of sample. Both shapes centred upon mean shape (not shown). c. Plot of PC2 coefficients of x-, y-, and z-coordinates of landmarks against landmark number, for median landmarks and those upon the right side of the dermatocranium



(Figs. 10c, 11 c, 12c.) can be considered to be independent of one another from PC to PC. Any consistencies in grouping across components are arrived at independently (insofar as this is possible, given the necessary integration

of the dermatocranium as a whole). However, the differences in the amount of sex- and allometry-free variance explained by each principal component (Table 3) requires weighting of the divisions suggested by each (Figs. 10c,

Fig. 12 Dorsal (a) and right lateral (b) wireframe reconstructions of dermatocranial shape showing the shape changes associated with PC3 from principal component analysis of SAFL data for *Phrynosoma hernandesi* sample. Shape at smallest PC3 value superimposed upon shape at largest PC3 value; red wireframe with dark grey fill—at smallest PC3 score of sample; black wireframe with blue fill—at largest PC3 score of sample. Both shapes centred upon mean shape (not shown). **c** Plot of PC3 coefficients of x-, y-, and z-coordinates of landmarks against landmark number, for median landmarks and those upon the right side of the dermatocranium



11c, 12c). Thus, the landmark groupings suggested by the coefficients of PC1 (Fig. 10c), that explains 24.287% of the total sex- and allometry-free variance in dermatocranial shape (Table 3), are considered to be stronger expressions of the regional consonance of variance in dermatocranial shape than are the landmark groupings suggested by the coefficients of the remaining retained PCs (Figs. 11c, 12c), which collectively explain 17.956% of the total sex- and allometry-free variance in dermatocranial shape (Table 3).

Discussion

We have demonstrated that, although there is no sexual dimorphism in the allometric relationship between landmark configuration centroid size and body size in *Phrynosoma hernandesi*, the species does display a small amount of dermatocranial sexual shape dimorphism. From our analysis, it is evident that the allometric integration of the dermatocranium of *P. hernandesi* through ontogeny is not simple. Sex- and allometry-free shape is characterized most markedly by variance in the area defined by the anterior portions of the squamosals, the ventral regions of the postorbitals, and the posterior processes of the jugals.

Ontogenetic Shape Change

Multivariate regression is not sensitive to the number of dependent variables (Mitteroecker and Gunz 2009), and so

the greater number of landmark coordinates than specimens in our sample will not invalidate our analyses of ontogenetic shape change.

Our sample consists of cross-sectional ontogenetic data (Cock 1966). Characterizations of ontogenetic shape change are thus inferential, as they are not derived from longitudinal records of actual relative landmark movement in individual lizards.

Slightly more than half of the variance of the symmetric portion of the Procrustes-fitted landmark data for both sexes of *Phrynosoma hernandesi* was explained by the regression of these data on $\ln(\text{centroid size})$. The lizard head is a complex structure, subject to a variety of selective forces (Kaliontzopoulou et al. 2008; Lazić et al. 2015). However, the predominance of centroid size, and thus lizard body size, in accounting for variance in dermatocranial shape in both sexes of *P. hernandesi* suggests that selective forces affecting dermatocranial shape may act principally through their effects on lizard size.

On the basis of external measurements, it has been demonstrated that the head of *Phrynosoma hernandesi* increases in width at a greater rate than it increases in length, with increasing body size (Powell and Russell 1985a). External measurements indicate geographical variation in the relative widths of the head in the regions of the lateral edges of the squamosals and the posterior portions of the jugals (Smith 1946; Reeve 1952; Montanucci 2015). Such morphological variation may reflect differing patterns of allometric growth among regions of the dermatocranium

(Crane 1993), suggesting that dermatocranial allometry is not simple in this species. Our results (Figs. 4, 5) indicate that this is the case.

The amount of variance in dermatocranial shape explained by sex is minimal (Table 2a). Adult male dermatocranial shape resembles in most respects that to be expected of a subadult female of the same body size (Fig. 6a, b). The regression coefficients of the two sexes follow very similar patterns over the landmark configuration (Fig. 7a, b). For these reasons, we will restrict our general discussion of ontogenetic shape change in *Phrynosoma hernandesi* to that exhibited by the female dermatocranium. Females in any case reach a greater adult size than do males (Fig. 2; Powell and Russell 1985a), and the results of allometric trends will be more easily visualized for females (Figs. 4a, b, 5a, b). Sexual shape dimorphism is discussed at greater length below.

Ontogenetic shape changes result in a broader, flatter posterior dermatocranium, with a marked emargination of its posterior border, a serrated posterolateral margin, and more prominent supraocular horns (Fig. 4a, b). The posterior superciliary processes of the prefrontals and the anterior superciliary processes of the frontal occlude larger portions of the lateral margins of the supraorbital fenestrae (Fig. 4a, b). The most prominent dermatocranial shape changes thus result in an increase in the amount of bone in the vicinities of the orbits and supraorbital fenestrae, and, laterally, of the braincase (Fig. 4a, b).

The dermatocranial horn array typical of *Phrynosoma* species (Fig. 1) is generally considered to constitute a defence for the head, and a deterrent to gape-limited predators (Pianka and Parker 1975; Sherbrooke 1991, 2003, 2008, 2013; Bergmann et al. 2009; Cooper and Sherbrooke 2010; Bergmann and Berk 2012). This has been demonstrated for some longer-horned species (Sherbrooke 1987, 2003; Young et al. 2004). The defensive strategies of the various species of *Phrynosoma*, however, are complex and do not rely solely upon the dermatocranial horn array (Sherbrooke 2013). The squamosal and supraocular horns of *P. hernandesi* are small in comparison to those of most of its congeners (Fig. 1p), and it does not appear to rely upon them for defence (Cope 1892; Smith 1946; Milne and Milne 1950; Sherbrooke 1987, 2003; Sherbrooke and Greenfield 2002; Sherbrooke et al. 2002). However, the expansion of the lateral margins of the dermatocranium and increase in size and elevation of the anterior superciliary processes of the frontal may serve as a defence against predators which attack the braincase and orbits. Grasshopper mice (*Onychomys*) have been shown to attack *P. cornutum* and *P. modestum* in this way (Sherbrooke 1991). *O. leucogaster* co-occurs with *P. hernandesi* in Canada (Soper 1964). Individual lizards that have sustained damage to the head consistent with survival of such attacks have been

observed in the Alberta populations of *P. hernandesi*. We thus hypothesize that the ontogenetic changes in dermatocranial shape typical of *P. hernandesi* produce a dermatocranial shape structured so as to protect the orbits and braincase against the kind of attacks mounted by rodents of the genus *Onychomys*, and any other predators which attack *P. hernandesi* in similar ways.

The amount of dermatocranial shape variance explained by size in both sexes (Table 2b, c) is consistent with this hypothesis. Cranial defences in species of *Phrynosoma* are thought to be more effective in larger individuals (Bergmann and Berk 2012). If predation exerts a strong selective pressure upon dermatocranial shape in *P. hernandesi*, we can expect dermatocranial shape to covary strongly with body size, particularly in the regions of the dermatocranium which we hypothesize function in protection of the orbits and braincase.

Complex ontogenetic dermatocranial changes in shape (Fig. 4a, b) take place over an almost-threefold increase in head length. Allometry can serve to integrate a structure over an ontogenetic size range (Olsen and Miller 1959; Jamniczky and Hallgrímsson 2009; Klingenberg 2008, 2009, 2013; Lazić et al. 2015). The allometric changes in shape defined by the multivariate regressions of the symmetric portions of the landmark configurations on $\ln(\text{centroid size})$ (Fig. 4a, b) must be considered in terms of all of the landmarks constituting the configurations (Márquez et al. 2012). However, the movements of landmarks described by the regression define shape change. It is evident from Fig. 7a, b that there are groups of contiguous landmarks exhibiting consonance in sign, and to a lesser degree magnitude. These groups are indicative of greater landmark movements, and hence greater shape change, in the areas of the dermatocranium that they cover, compared to those covering other regions. This localization of consonant movement is most marked in the landmarks covering the transverse posterolateral processes of the frontal, those covering the ventral margins of the postorbital and the anterior regions of the squamosals, those covering the posterolateral extremities of the parietal, those covering the medial portion of the posterior margin of the parietal, and those covering the inferior processes of the squamosals (Fig. 8). Allometric shape change as described by the multivariate regressions for each sex is not evenly distributed over the dermatocranium (Fig. 7a, b), which suggests that there may be inhomogeneities in the dermatocranium's allometric integration.

Allometric shape change in the lizard head has chiefly been examined by means of geometric morphometric methods in lacertids, and in this group primarily involves a greater increase in size of the posterior region of the head relative to the anterior region (Bruner and Costantini 2007; Kaliontzopoulou 2011; Kaliontzopoulou et al. 2008;

Ljubisavljević et al. 2010; Urošević et al. 2013; Lazić et al. 2015). Allometric integration as complex as that proposed for *Phrynosoma hernandesi* (Fig. 6) has not been reported for other lizard species.

If the landmarks grouped by regression coefficient consonance (Figs. 7, 8) represent regions of inhomogeneity within the allometric integration of the dermatocranium, then overall allometric integration of the dermatocranium will be weaker than it would be if they did not exist. Without comparative data from other species of *Phrynosoma*, it is not possible to evaluate this hypothesis. However, weaker overall integration has been associated with greater morphological disparity within some groups (Goswami and Polly 2010; Goswami et al. 2014; Haber 2016). The species of *Phrynosoma* display wide disparity in dermatocranial morphology (Fig. 1; Reeve 1952; Presch 1969; Montanucci 1987; Baur and Montanucci 1998; Sherbrooke 2003), and the complex allometric patterning of *P. hernandesi*, a highly-derived species (Leaché and McGuire 2006; Nieto-Montes de Oca et al. 2014; Leaché and Linkem 2015) suggests that spatially inhomogeneous allometric integration of the dermatocranium may be associated with this disparity. This hypothesis must be tested with comparative data; it is beyond the scope of this study.

Sexual Shape Dimorphism

Sexual dimorphism in head shape produced by differences in ontogenetic trajectory have been demonstrated, using geometric morphometric techniques, for a number of lizard species (Kaliontzopoulou 2011; Kaliontzopoulou et al. 2007, 2008, 2010; Ljubisavljević et al. 2010; Piras et al. 2011; Sacchi et al. 2015; Sanger et al. 2013; Urošević et al. 2013; Zuffi et al. 2011). Such dimorphism is generally associated with sexual differences in head morphology associated with biting ability, and is found in species in which males contest for mating opportunities (Kaliontzopoulou 2011; Kaliontzopoulou et al. 2007, 2008, 2010; Ljubisavljević et al. 2010; Piras et al. 2011; Sacchi et al. 2015; Sanger et al. 2013; Urošević et al. 2013). Sexual shape dimorphism of the head may be the result of differences in allometric trajectory between the sexes (Kaliontzopoulou 2011; Kaliontzopoulou et al. 2007, 2008). It may also be the product of such allometric sexual differences in addition to sexual shape dimorphism not associated with allometry (Ljubisavljević et al. 2010), or of truncation of growth in one sex along a common allometric trajectory (Kaliontzopoulou 2011; Zuffi et al. 2011).

The ontogenetic sexual difference in dermatocranial shape displayed by *Phrynosoma hernandesi*, while statistically significant (Table 2), produces male and female dermatocranial shapes differing minimally at the largest male centroid size (Fig. 6a, b). The ontogenetic relationship

between centroid size and body length does not differ between the sexes (Online Resource, Fig. S-2, Table S-2), and so differences in centroid size must result from very small contributions from sexual shape dimorphism, as is indicated in Table 2. This lack of sexual dimorphism in the scaling of landmark configuration size to body size means that a comparison of dermatocranial shape at a common centroid size constitutes a comparison of dermatocranial shape at the same body size. Body size has been shown to be associated with ecological differences between the sexes in these populations (Powell and Russell 1984, 1985b). Such comparisons may permit some explanations of the sexual shape dimorphism described here, although none immediately suggest themselves. It is unlikely that the slight anterior projection of the anterior margin of the rostrum in males at the greatest common centroid size (Fig. 6a, b) is of any consequence in prey handling, and in fact it has been shown that there is no difference in prey size taken by adult males and comparably sized subadult females (Powell and Russell 1984). Similarly, no immediate functional significance suggests itself for the slight posterior movement of the transverse posterolateral processes of the frontal, and the horns that they bear (F_0), in males relative to females (Fig. 6b). The mating strategy of this species does not feature territoriality or male–male agonistic interactions (Lynn 1965; Powell and Russell 1985a; Zamudio 1998; Bergmann and Berk 2012), and so slightly more prominent supraocular horns in adult males are unlikely to be of significance in this regard.

Powell and Russell (1985a) hypothesized that body growth in males is truncated relative to that of females, producing the sexual size dimorphism characteristic of the populations of *Phrynosoma hernandesi* represented by our present sample. Characteristic SVL growth rates do not differ significantly between the sexes (Powell and Russell 1985a), which supports this hypothesis. Given this, the sexual shape dimorphism in dermatocranial shape that we describe here (Fig. 6a, b) does not appear to be a consequence of heterochrony.

We must reject our hypothesis that male dermatocranial shape is a simple consequence of truncation of growth in body size relative to that of females. However, the significance of the sexual shape dimorphism described here, if there is any, remains obscure.

Sex- and Allometry-Free Shape Variation

Dermatocranial shape change explained by PC1 is most strongly expressed in the regions of the tripartite sutures formed between the posterior processes of the jugals, the anterior regions of the squamosals, and the ventral regions of the postorbitals (Fig. 10a, b), where the dermatocranium attains its greatest breadth (Fig. 3a). The most

marked shape changes described by PC1 involve dorso-ventral and medio-lateral movements of this region of the dermatocranium. At the smallest PC1 score, this produces a dermatocranial shape that is dorso-ventrally compressed, with laterally expanded margins in the region of the triradiate suture, and that is compressed along the antero-posterior axis (Fig. 10a, b). At the greatest PC1 score, dermatocranial shape is dorso-ventrally expanded and medially compressed in the region of the tripartite suture, with an extended rostrum and posterior margin, and an elevated cranial table (Fig. 10a, b). Superficially, the dermatocranium appears to flex dorso-ventrally in the region of the triradiate sutures over the PC1 score range (Fig. 10b).

The principle shape changes described by PC2 are a minor change in dorso-ventral compression of the dermatocranium and elevation of the transverse posterolateral processes of the frontal, together with extension or retraction of the anterior margin of the rostrum (Fig. 11a, b). Those described by PC3 consist primarily of anterior or posterior movement of the inferior processes of the squamosals, together with depression or elevation of the post-rostral dermatocranial roof (Fig. 12a, b). These PCs combined explain less variance than does PC1 (Table 3), and these shape changes are hence of less consequence.

The localization of the shape change explained by PC1 is also evident in the consonance of magnitude and size displayed by PC1 coefficients over the landmark configuration (Fig. 10c). Subsets of landmarks within a configuration are not adequate to capture local variation in shape in the areas that they cover (Márquez et al. 2012). Thus these regions of PC1 coefficient consonance cannot be taken as displaying greater covariance within themselves than they do with the remainder of the landmark configuration, without further investigation. However, interpreted as indications of shape change, they do suggest that the variance delimited by PC1 is chiefly expressed in the region of the triradiate suture joining the posterior processes of the jugals, the ventral regions of the postorbitals, and the anterior regions of the squamosals. A large part of the shape variance common to both sexes of *Phrynosoma hernandesi* is thus associated with breadth and degree of dorso-ventral compression of the posterior portion of the dermatocranium, and the antero-posterior extension or retraction of the whole (Fig. 10a, b).

The dermatocranial change described by the principal component analysis is that common to both males and females in the absence of allometric integration. However, the analysis of ontogenetic shape change incorporated this variance, and so the shape changes revealed by the two analyses cannot be considered to be independent. Both the analysis of ontogenetic shape change and the analysis of the SSAFL data indicated that dermatocranial shape change,

while distributed over the dermatocranium, is most marked in its posterior region.

Summary and Conclusions

We examined shape and shape variation in the dermatocranium of the Greater Short-horned Lizard (*Phrynosoma hernandesi*) through geometric morphometric methods. We found that this species does display a small degree of sexual shape dimorphism due to allometric differences between the sexes, leading to rejection of our first hypothesis, that there is no sexual difference in allometric trajectory of dermatocranial shape. Adult male dermatocranial shape is not produced by earlier truncation of growth along a common allometric trajectory, although sexual shape differences at the greatest common body size are small.

Over half of the shape variation in both sexes is attributable to allometry. Integration of the dermatocranium through allometry produces complex shape changes, and ontogenetic shape change is most marked in portions of the posterior region of the dermatocranium. We thus fail to reject our second hypothesis, that changes in dermatocranial shape over the ontogenetic size range are produced by differences in rate of shape change among the different regions of the dermatocranium, particularly between the anterior and posterior portions of the dermatocranium.

Sex- and allometry-free shape variance, examined through principal component analysis, is concentrated in a few dimensions. Shape variance is concentrated in the anterior regions of the squamosals and posterior regions of the jugals, and the posterior sector of the parietal. We thus corroborate our third hypothesis, of uneven distribution of dermatocranial shape variance over the dermatocranium of *Phrynosoma hernandesi* in the absence of the variance attributable to allometry.

Both allometric integration and sex- and allometry-free variance contribute to the final shape of the dermatocranium. This final shape is consistent with passive defence against predators which attack the braincase and orbits.

We hypothesize, on the basis of the results presented here, that the complexity of dermatocranial shape change and shape variance defined here for *Phrynosoma hernandesi* is indicative of dermatocranial modularity. Further analysis is required to test this hypothesis.

We hypothesize that, if this is phylogenetically conserved among the species of *Phrynosoma*, it would serve as an explanation for the dermatocranial and horn disparity observed among the species of *Phrynosoma* (Fig. 1), permitting evolvability of the dermatocranium by breaking constraints on shape. Phylogenetic analysis of variation in dermatocranial shape will be necessary to test this hypothesis.

Acknowledgements Support for this project came from a National Science and Engineering Research Council Discovery Grant to APR, National Institute of Health grant 2R01DE019638 and National Science and Engineering Research Council Grant #238992-12 to BH, and a Queen Elizabeth II Doctoral Scholarship to GLP. We thank the following for loans of specimens of *Phrynosoma hernandesi* under their care: C. Pazkowski (University of Alberta Museum of Zoology), W. Fitch (University of Calgary Museum of Zoology), R. Murphy (Royal Ontario Museum), M. Steigerwald (Canadian Museum of Nature), M. Steinhilber (Royal Alberta Museum), and R. Poulin (Royal Saskatchewan Museum). We are grateful to C.J. Franklin (University of Texas at Arlington), J. Vindum (California Academy of Sciences), C.L. Spencer (University of Californian Museum of Vertebrate Zoology), G. Schneider (University of Michigan Museum of Zoology), J.R. Dixon (Texas Cooperative Wildlife Collection), G. Bradley (University of Arizona), and K. de Queiroz (United States National Museum of Natural History) for loans of specimens of other species of *Phrynosoma* illustrated here. We are greatly indebted to H. Buie, W. Lu, and A. Tinius for technical assistance. E. Sherratt, M.L. Zelditch, and D.C. Adams provided critical help with geomorph. We thank A. Haber and an anonymous reviewer for comments which resulted in a greatly improved final product.

Compliance with Ethical Standards

Conflict of interest The authors declare that they have no conflict of interest.

References

- Adams, D. C., & Otárola-Castillo, E. (2013). Geomorph: an R package for the collection and analysis of geometric morphometric shape data. *Methods in Ecology and Evolution*, 4, 393–399.
- Adams, D. C., Otárola-Castillo, E. & Sherratt, E. (2014) *Geomorph*: Software for geometric morphometric analyses. R package version 2.0. <http://cran.r-project.org/web/packages/geomorph/index.html>.
- Baur, B. E., & Montanucci, R. R. (1998). *Krötenechsen*. Munich: Offenbach: Herpeton, Verlag Elke Köhler.
- Bergmann, P. J., & Berk, C. P. (2012). The evolution of positive allometry of weaponry in horned lizards (*Phrynosoma*). *Evolutionary Biology*, 39, 311–323.
- Bergmann, P. J., Meyers, J. J., & Irschick, D. J. (2009). Directional evolution of stockiness coevolves with ecology and locomotion in lizards. *Evolution*, 63, 215–227.
- Bookstein, F. L. (1991). *Morphometric Tools for landmark data. Geometry and biology*. Cambridge: Cambridge University Press.
- Bruner, E., & Costantini, D. (2007). Head morphological variation in *Podarcis muralis* and *Podarcis sicula*: A landmark-based approach. *Amphibia-Reptilia*, 28, 566–573.
- Bryant, H.C. (1911) The horned lizards of California and Nevada of the genera *Phrynosoma* and *Anota*. *University of California Publications in Zoology*, 9, 1–84.
- Cock, A. G. (1966). Genetical aspects of metrical growth and form in animals. *Quarterly Review of Biology*, 41, 131–190.
- Collyer, M. L., Sekora, D. J., & Adams, D. C. (2015). A method for analysis of phenotypic change for phenotypes described by high-dimensional data. *Heredity*, 115, 357–365.
- Cooper, W. E. J., & Sherbrooke, W. C. (2010). Plesiomorphic escape decisions in cryptic horned lizards (*Phrynosoma*) having highly derived antipredatory defenses. *Ethology*, 116, 920–928.
- Cope, E. D. (1892). The osteology of the Lacertilia. *Proceedings of the American Philosophical Society*, 30, 185–221.
- Crane, W. P. (1993). The ontogeny of postcranial integration in the Common Tern *Sterna hirundo*. *Evolution*, 47, 1138–1151.
- Etheridge, R. (1964) The skeletal morphology and systematic relationships of sceloporine lizards. *Copeia*, 1964, 610–631.
- Evans, S. E. (2008) The skull of lizards and tuatara. In: C. Gans, A. S. Gaunt & K. Adler (Eds.), *Biology of the Reptilia Morphology H. The Skull of Lepidosauria* (Vol. 20, pp. 1–347). Ithaca, NY: Society for the Study of Amphibians and Reptiles.
- Goodall, C. (1991). Procrustes methods in the statistical analysis of shape. *Journal of the Royal Statistical Society. Series B*, 53, 285–339.
- Goswami, A., & Polly, P. D. (2010). The influence of modularity on cranial morphological disparity in Carnivora and Primates (Mammalia). *PLoS ONE*, 5, e9517.
- Goswami, A., Smaers, J. B., Soligo, C., & Polly, P. D. (2014). The macroevolutionary consequences of phenotypic integration: from development to deep time. *Philosophical Transactions of the Royal Society B: Biological Sciences*, 369, 20130254.
- Haber, A. (2016). Phenotypic covariation and morphological diversification in the ruminant skull. *American Naturalist*, 187, 576–591.
- Jamniczky, H. A., & Hallgrímsson, B. (2009). A comparison of covariance structure in wild and laboratory muroid crania. *Evolution*, 63, 1540–1556.
- Jenkins, R. L., & Tanner, W. W. (1968). Osteology and myology of *Phrynosoma p. platyrhinos* Girard and *Phrynosoma d. hernandesi* Girard. *Brigham Young University Science Bulletin Biological Series*, 9, 1–34.
- Jollie, M. T. (1960). The head skeleton of the lizard. *Acta Zoologica*, 41, 1–64.
- Kalioztopoulou, A. (2011). Geometric morphometrics in herpetology: modern tools for enhancing the study of morphological variation in amphibians and reptiles. *Basic and Applied Herpetology*, 25, 5–32.
- Kalioztopoulou, A., Carretero, M. A., & Llorente, G. A. (2010). Intraspecific ecomorphological variation: linear and geometric morphometrics reveal habitat-related patterns within *Podarcis bocagei* wall lizards. *Journal of Evolutionary Biology*, 23, 1234–1244.
- Kalioztopoulou, A., Carretero, M. M., & Llorente, G. A. (2007). Multivariate and geometric morphometrics in the analysis of sexual dimorphism variation in *Podarcis* lizards. *Journal of Morphology*, 268, 152–165.
- Kalioztopoulou, A., Carretero, M. M., & Llorente, G. A. (2008). Head shape allometry and proximate causes of head sexual dimorphism in *Podarcis* lizards: Joining linear and geometric morphometrics. *Biological Journal of the Linnean Society*, 93, 111–124.
- Klingenberg, C. P. (2008). Morphological integration and developmental modularity. *Annual Review of Ecology, Evolution and Systematics*, 39, 115–132.
- Klingenberg, C. P. (2009). Morphometric integration and modularity in configurations of landmarks: tools for evaluating *a priori* hypotheses. *Evolution and Development*, 11, 405–421.
- Klingenberg, C. P. (2011). MorphoJ: An integrated software package for geometric morphometrics. *Molecular Ecology Resources*, 11, 353–357.
- Klingenberg, C. P. (2013). Cranial integration and modularity: Insights into evolution and development from morphometric data. *Hystrix*, 24, 43–58.
- Klingenberg, C. P., Barluenga, M., & Meyer, A. (2002). Shape analysis of symmetric structures: Quantifying variation among individuals and asymmetry. *Evolution*, 56, 1909–1920.
- Lazić, M. M., Carretero, M. A., Crnobrnja-Isailović, J., & Kalioztopoulou, A. (2015). Effects of environmental disturbance on phenotypic variation: an integrated assessment of canalization,

- developmental stability, modularity, and allometry in lizard head shape. *The American Naturalist*, 185, 44–58.
- Leaché, A. D., & Linkem, C. W. (2015). Phylogenomics of horned lizards (Genus: *Phrynosoma*) using targeted sequence capture data. *Copeia*, 103, 586–594.
- Leaché, A. D., & McGuire, J. A. (2006). Phylogenetic relationships of horned lizards (*Phrynosoma*) based on nuclear and mitochondrial data: Evidence for a misleading mitochondrial gene tree. *Molecular Phylogenetics and Evolution*, 39, 628–644.
- Leung, M. N.-Y., Paszkowski, C. A., & Russell, A. P. (2014). Genetic structure of the endangered greater short-horned lizard (*Phrynosoma hernandesi*) in Canada: Evidence from mitochondrial and nuclear genes. *Canadian Journal of Zoology*, 92, 875–883.
- Ljubicavljević, K., Urošević, A., Aleksić, I., & Ivanović, A. (2010). Sexual dimorphism of skull shape in a lacertid lizard species (*Podarcis* spp., *Dalmatolacerta* spp., *Dinarolacerta* spp.) revealed by geometric morphometrics. *Zoology*, 113, 168–174.
- Lynn, R. T. (1965). A comparative study of display behavior in *Phrynosoma* (Iguanidae). *The Southwestern Naturalist*, 10, 25–30.
- Márquez, E. J., Cabeen, R., Woods, R. P., & Houle, D. (2012). The measurement of local variation in shape. *Evolutionary Biology*, 39, 419–439.
- Milne, L. J., & Milne, M. J. (1950). Notes on the behavior of horned toads. *American Midland Naturalist*, 44, 720–741.
- Mitteroecker, P., & Gunz, P. (2009). Advances in geometric morphometrics. *Evolutionary Biology*, 36, 235–247.
- Mitteroecker, P., Gunz, P., Windhager, S., & Schaefer, K. (2013). A brief review of shape, form, and allometry in geometric morphometrics, with applications to human facial morphology. *Hystrix*, 24, 59–66.
- Montanucci, R. R. (1987). A phylogenetic study of the horned lizards, genus *Phrynosoma*, based upon skeletal and external morphology. *Natural History Museum of Los Angeles County Contributions in Science*, 390, 1–36.
- Montanucci, R. R. (2015). A taxonomic revision of the *Phrynosoma douglassii* species complex (Squamata: Phrynosomatidae). *Zootaxa*, 4015, 1–177.
- Montanucci, R. R., & Baur, B. E. (1982). Mating and courtship-related behaviors of the short-horned lizard, *Phrynosoma douglassii*. *Copeia*, 1982, 971–974.
- Monteiro, L. R., & Abe, A. S. (1997). Allometry and morphological integration in the skull of *Tupinambis merianae* (Lacertilia: Tupinambidae). *Amphibia-Reptilia*, 18, 397–405.
- Nieto-Montes de Oca, A., Arenas-Moreno, D., Beltrán-Sánchez, E., & Leaché, A. D. (2014). A new species of horned lizard (Genus *Phrynosoma*) from Guerrero, México, with an updated multilocus phylogeny. *Herpetologica*, 70, 241–257.
- Pianka, R. E. & Parker, W. S. (1975) Ecology of horned lizards: a review with special reference to *Phrynosoma platyrhinos*. *Copeia*, 1975, 141–162.
- Piras, P., Salvi, D., Ferrara, G., Maiorino, L., Delfino, M., Pedde, L., & Kotsakis, T. (2011). The role of post-natal ontogeny in the evolution of phenotypic diversity in *Podarcis* lizards. *Journal of Evolutionary Biology*, 24, 2705–2720.
- Powell, G. L., & Russell, A. P. (1984). The diet of the eastern short-horned lizard (*Phrynosoma douglassii brevirostre*) in Alberta and its relationship to sexual size dimorphism. *Canadian Journal of Zoology*, 62, 428–440.
- Powell, G. L., & Russell, A. P. (1985a). Growth and sexual size dimorphism in Alberta populations of the eastern short-horned lizard, *Phrynosoma douglassii brevirostre*. *Canadian Journal of Zoology*, 63, 139–154.
- Powell, G. L., & Russell, A. P. (1985b). Field thermal ecology of the eastern short-horned lizard (*Phrynosoma douglassii brevirostre*) in southern Alberta. *Canadian Journal of Zoology*, 63(228 –), 238.
- Powell, G. L., & Russell, A. P. (1991). Parturition and clutch characteristics of short-horned lizards (*Phrynosoma douglassii brevirostre*) from Alberta. *Canadian Journal of Zoology*, 69, 2759–2764.
- Powell, G. L., Russell, A. P., & Ryan, M. J. (2002). Ontogenetic scaling of the cranial horn array in *Phrynosoma orbiculare* (Squamata: Phrynosomatidae). *Journal of Herpetology*, 36, 578–589.
- Powell, G. L. (2016) Evolution of dermatocranial shape in horned lizards (*Phrynosoma*). Unpubl. Doctoral Thesis, University of Calgary, May 2016.
- Presch, W. (1969) Evolutionary osteology and relationships of the horned lizard genus *Phrynosoma* (family Iguanidae). *Copeia*, 1969, 250–275.
- R Development Core Team (2013) *R: a language and environment for statistical computing*. Version 3.0.1. R Vienna: Foundation for Statistical Computing. <http://cran.Rproject.org>.
- Reeve, W. L. (1952). Taxonomy and distribution of the horned lizard genus, *Phrynosoma*. *The University of Kansas Science Bulletin*, 34, 817–960.
- Sanger, T. J., Mahler, D. L., Abzhanov, A., & Losos, J. B. (2011). Roles for modularity and constraint in the evolution of cranial diversity among *Anolis* lizards. *Evolution*, 66, 1525–1542.
- Sanger, T. J., Sherratt, E., McGlothlin, J. W., Brodie, E. D., Losos, J. B., & Abzhanov, A. (2013). Convergent evolution of sexual dimorphism in skull shape using distinct developmental strategies. *Evolution*, 67, 2180–2193.
- Sherbrooke, W. C. (1987). Defensive head posture in horned lizards (*Phrynosoma*: Sauria: Iguanidae). *The Southwestern Naturalist*, 32, 512–515.
- Sherbrooke, W. C. (1991). Behavioral (predator-prey) interactions of captive grasshopper mice (*Onychomys torridus*) and horned lizards (*Phrynosoma cornutum* and *P. modestum*). *American Midland Naturalist*, 126, 187–195.
- Sherbrooke, W. C. (2003). *Introduction to horned lizards of North America*. Berkeley: University of California Press.
- Sherbrooke, W. C. (2008). Antipredator responses by Texas horned lizards to two snake taxa with different foraging and subjugation strategies. *Journal of Herpetology*, 42, 145–152.
- Sherbrooke, W. C. (2013). Horned lizard responses to diverse threats from diverse predators: Mental constructs and cognitive worlds? In Lutterschmidt W. I. (Ed.), *Reptiles in research: investigations of ecology, physiology, and behavior from desert to sea* (pp. 177–195). Hauppauge, NY: Nova.
- Sherbrooke, W. C., Brown, E. R., & Brown, J. L. (2002). *Phrynosoma hernandesi* (Short-horned Lizard). Successful open-mouthed threat defense. *Herpetological Review*, 33, 208.
- Sherbrooke, W. C., & Greenfield, M. D. (2002). *Phrynosoma hernandesi* (Short-horned Lizard). Defensive hiss. *Herpetological Review*, 33, 208–209.
- Slice, D. E. (2007). Geometric morphometrics. *Annual Review of Anthropology*, 36, 261–281.
- Smith, H. M. (1946). *Handbook of lizards. Lizards of the United States and of Canada*. Ithaca, NY: Comstock Publishing Company Inc.
- Soper, J. D. (1964). *The Mammals of Alberta*. Edmonton: The Hamly Press Ltd.
- Urošević, A., Ljubicavljević, K., & Ivanović, A. (2013). Patterns of cranial ontogeny in lacertid lizards: morphological and allometric disparity. *Journal of Evolutionary Biology*, 26, 399–415.
- Young, K. V., Brodie, E. D. Jr., & Brodie, E. D. (2004). How the horned lizard got its horns. *Science*, 304, 65.
- Zamudio, K. R. (1998). The evolution of female-biased sexual size dimorphism: a population-level comparative study in horned lizards (*Phrynosoma*). *Evolution*, 52, 1821–1833.

- Zamudio, K. R., Jones, K. B., & Ward, R. H. (1997). Molecular systematics of short-horned lizards: biogeography and taxonomy of a widespread species complex. *Systematic Biology*, *46*, 284–305.
- Zelditch, M. L., Swiderski, D. L., Sheets, H. D., & Fink, W. L. (2004). *Geometric morphometrics for biologists. A primer*. San Diego, CA: Elsevier Academic Press.
- Zuffi, M. A. L., Sacchi, R., Pupin, F., & Cencetti, T. (2011). Sexual size and shape dimorphism in the Moorish gecko (*Tarentola mauretana*, Gekkota, Phyllodactylidae). *North-Western Journal of Zoology*, *7*, 189–197.